nature COMMUNICATIONS

ARTICLE

Received 29 Jan 2014 | Accepted 21 Jul 2014 | Published 27 Aug 2014

DOI: 10.1038/ncomms5770

Recurrent *CDC25C* mutations drive malignant transformation in FPD/AML

Akihide Yoshimi[1,*], Takashi Toya[1,*], Masahito Kawazu[2], Toshihide Ueno[3], Ayato Tsukamoto[1], Hiromitsu Iizuka[1], Masahiro Nakagawa[1], Yasuhito Nannya[1], Shunya Arai[1], Hironori Harada[4], Kensuke Usuki[5], Yasuhide Hayashi[6], Etsuro Ito[7], Keita Kirito[8], Hideaki Nakajima[9], Motoshi Ichikawa[1], Hiroyuki Mano[3] & Mineo Kurokawa[1]

Familial platelet disorder (FPD) with predisposition to acute myelogenous leukaemia (AML) is characterized by platelet defects with a propensity for the development of haematological malignancies. Its molecular pathogenesis is poorly understood, except for the role of germline *RUNX1* mutations. Here we show that *CDC25C* mutations are frequently found in FPD/AML patients (53%). Mutated CDC25C disrupts the G2/M checkpoint and promotes cell cycle progression even in the presence of DNA damage, suggesting a critical role for CDC25C in malignant transformation in FPD/AML. The predicted hierarchical architecture shows that *CDC25C* mutations define a founding pre-leukaemic clone, followed by stepwise acquisition of subclonal mutations that contribute to leukaemia progression. In three of seven individuals with *CDC25C* mutations, *GATA2* is the target of subsequent mutation. Thus, *CDC25C* is a novel gene target identified in haematological malignancies. *CDC25C* is also useful as a clinical biomarker that predicts progression of FPD/AML in the early stage.

[1] Department of Hematology and Oncology, Graduate School of Medicine, The University of Tokyo, 7-3-1 Hongo, Bunkyo-ku, Tokyo 113-8655, Japan. [2] Department of Medical Genomics, Graduate School of Medicine, The University of Tokyo, 7-3-1 Hongo, Bunkyo-ku, Tokyo 113-8655, Japan. [3] Department of Cellular Signaling, Graduate School of Medicine, The University of Tokyo, 7-3-1 Hongo, Bunkyo-ku, Tokyo 113-8655, Japan. [4] Department of Hematology, Juntendo University School of Medicine, 3-1-3 Hongo, Bunkyo-ku, Tokyo 113-8431, Japan. [5] Department of Hematology, NTT Medical Center Tokyo, 5-9-22 Higashi-Gotanda, Shinagawa-ku, Tokyo 141-8625, Japan. [6] Department of Hematology/Oncology, Gunma Children's Medical Center, 779 Simohakoda, Kitaakebonocho, Shibukawa-shi, Gunma 377-8577, Japan. [7] Department of Pediatrics, Graduate School of Medicine, Hirosaki University, 53 Honmachi, Hirosaki-shi, Aomori 036-8563, Japan. [8] Department of Hematology and Oncology, University of Yamanashi, 1110 Simokawakita, Chuou-shi, Yamanashi 409-3898, Japan. [9] Division of Hematology, Department of Internal Medicine, Keio University School of Medicine, 35 Shinanomachi, Shinjyuku-ku, Tokyo 160-8582, Japan. * These authors contributed equally to this work. Correspondence and requests for materials should be addressed to M.K. (email: kurokawa-tky@umin.ac.jp).

Familial platelet disorder (FPD)/acute myelogenous leukaemia (AML) (MIM601399) is an autosomal dominant disorder with inherited thrombocytopenia, abnormal platelet function and a lifelong risk of the development of a variety of haematological malignancies[1], such as AML, myelodysplastic syndromes (MDS) and myeloproliferative neoplasms. Although inherited *RUNX1* mutations are the cause of the congenital thrombocytopenia, it remains unclear whether a mutation in *RUNX1*, which is generally known to have a dominant-negative effect[2–4], is sufficient to induce the development of haematological malignancies in individuals with FPD/AML. It is also not known whether additional gene mutations are required for the transformation, and, if so, which genes are involved. Given that only 40% of FPD/AML patients develop these neoplasms[5] and that a relatively long period is required for subsequent *RUNX1* mutation-mediated development of neoplasms in FPD/AML, the secondary genetic events may function as a driver to promote malignant transformation. We reasoned that identifying gene mutations responsible for the malignant transformation of FPD/AML would provide indispensable information for addressing these questions. However, only about 30 pedigrees with FPD/AML have been reported so far, and the rarity of this disorder has impeded the establishment of clinical diagnostic criteria and the clinical improvement to refine cancer therapy and to identify biomarkers that would allow detection of patients at risk for the onset of malignancies in FPD/AML.

We collected DNA samples and clinical information of 73 individuals, belonging to 57 pedigrees, who have a history of familial thrombocytopenia and/or haematological malignancies, with the aim of identifying pedigrees with FPD/AML and uncovering recurrent mutations that drive the malignant transformation. Next-generation sequencing and single-cell sequencing strategy suggest that somatic mutation in *CDC25C* may be one of the early genetic events for leukaemic initiation in FPD/AML, and further stepwise acquisition of mutations such as *GATA2* leads to FPD/AML-associated leukaemic progression. These observations shed light on a part of leukemogenesis in FPD/AML.

Results

A novel gene target in haematological disorders. Thirteen patients in 7 pedigrees were diagnosed as having FPD/AML after screening for germline *RUNX1* mutations in 73 index patients; 7 of the 13 patients had developed haematological malignancies, while the other 6 only showed thrombocytopenia (Table 1). Most of the detected *RUNX1* mutations were point mutation in Runt homology domain or frame-shift mutation that lost transactivation domain, consistent with the previous reports[2,4]. As haploinsufficiency of *RUNX1* might cause familial thrombocytopenia with propensity to develop AML[1], we also examined whether the pedigrees have *RUNX1* loss of heterozygosity (LOH) or not. A synchronized quantitative-PCR method[6] and single-nucleotide polymorphism (SNP) sequencing detected no case with LOH in *RUNX1* in our cohort (Supplementary Fig. 1 and detailed in Methods). To systematically identify additional genetic alterations, we utilized whole-exome sequencing for two individuals from the same FPD/AML pedigree who shared a common *RUNX1*_p.Phe303fs mutation and who had developed MDS (subject 20) or myelofibrosis (subject 21) at the age of 37 and 17 years, respectively. In both these patients, the disease had progressed to AML[7]. Validation by Sanger sequencing and/or targeted deep sequencing of candidate mutations in paired tumour/normal DNA samples confirmed 10 (subject 20) and 8 (subject 21) somatically acquired nonsynonymous mutations (Table 2; Supplementary Figs 2–4; Supplementary Methods). Surprisingly, both patients carried the identical somatic *CDC25C* mutation (p.Asp234Gly), which had not been reported previously in human cancers (Fig. 1a,b). Prompted by this finding, we investigated *CDC25C* mutations in other FPD/AML cases by deep sequencing. In total, four of seven affected patients with haematological malignancies had *CDC25C* mutations, of which three carried the same p.Asp234Gly mutation. Moreover, *CDC25C* mutations were detected in an additional three FPD/AML patients who had not yet developed haematological malignancies, although the variant allele fractions (VAFs) were much lower in this group of patients than in those who had already developed haematological malignancies (Fig. 1c; Table 1). Thus, 7 of the 13 FPD/AML patients (53%) harboured a *CDC25C* mutation. *CDC25C* was also screened for mutations in 90 sporadic MDS and 53 AML patients, including 13 MDS and 3 AML cases who carried *RUNX1* mutations. No *CDC25C* mutations were identified in the 90 sporadic cases, except for the p.Ala344Val in an MDS patient bearing a *RUNX1* mutation, indicating that *CDC25C* mutations were significantly associated with germline, but not with somatic *RUNX1* mutations ($P = 0.004$; Supplementary Fig. 5; Supplementary Table 1).

Clonal evolution of FPD/AML. Deep sequencing of individual mutations that had been detected by whole-exome sequencing

Table 1 | Mutational status of *CDC25C* in FPD/AML patients.

Pedigree number	Subject number	RUNX1 mutation	Disease status	Age, years*	CDC25C mutation	VAF (%)
18	20	p.Phe303fs	MDS/AML	37/38	p.Asp234Gly	31.7/45.8
	21		MF/AML	17/18	p.Asp234Gly	31.1/39.0
19	22	p.Arg174*	AML	41	p.His437Asn	39.7
54	65	p.Ser140Asn	MDS	25	—	—
	66		AML	56	p.Asp234Gly	24.2
32	38	p.Leu445Pro	HCL	72	—	—
16	18	p.Thr233fs	Thrombocytopenia	—	p.Asp234Gly	5.9
53	62	p.Gly262fs	MDS	12	—	—
	63		Thrombocytopenia	—	—	—
	67		Thrombocytopenia	—	—	—
57	71	p.Gly172Glu	Pancytopenia†	—	p.Asp234Gly	8.3
	72		Thrombocytopenia	—	—	—
	73		Thrombocytopenia	—	p.Lys233Glu	1.8

AML, acute myeloid leukemia; FPD, familial platelet disorder; HCL, hairy cell leukemia; MDS, myelodysplastic syndrome; MF, myelofibrosis; VAF, variant allele fraction.
*Age at the time of diagnosis of each haematological malignancy is shown.
†Thrombocytopenia, leukopenia and iron-deficiency anemia were diagnosed.

Table 2 | Validated somatic mutations.

Gene symbol	Ref seq_no.	Amino-acid change	Position (hg19)	Base change	Mutation type	SIFT prediction	VAF at MDS/MF (%)	VAF at AML (%)
Subject 20								
AGAP4	NM_133446	p.Arg484Cys	g.chr10:46321905	C->T	Missense	Damaging	13.2	11.5
CDC25C	NM_001790	p.Asp234Gly	g.chr5:137627720	A->G	Missense	Damaging	31.7	45.8
CHEK2	NM_007194	p.Arg406His	g.chr22:29091740	G->A	Missense	Tolerated	14.6	11.1
COL9A1	NM_001851	p.Gly878Val	g.chr6:70926733	G->T	Missense	Damaging	9.6	26.4
DTX2	NM_001102594	p.Pro74Arg	g.chr7:76110047	C->G	Missense	Damaging	18.3	11.2
FAM22G	NM_001170741	p.Ser508Thr	g.chr9:99700727	T->A	Missense	Tolerated	10.2	27.6
GATA2	NM_001145661	p.Leu321His	g.chr3:128202758	T->A	Missense	Damaging	0.0	28.1
LPP	NM_001167671	p.Val538Met	g.chr3:188590453	G->A	Missense	Damaging	9.7	28.8
RP1L1	NM_178857	p.Ser215fs	g.chr8:10480295	insC	Frameshift	Damaging	14.2	12.7
SIGLEC9	NM_014441	p.Ser437Gly	g.chr19:51633253	A->G	Missense	Tolerated	27.4	42.5
Subject 21								
ANXA8L1	NM_001098845	p.Val281Ala	g.chr10:48268018	T->C	Missense	Damaging	30.8	36.8
CDC25C	NM_001790	p.Asp234Gly	g.chr5:137627720	A->G	Missense	Damaging	31.1	39.1
DENND5A	NM_001243254	p.Arg320Ser	g.chr11:9215218	A->C	Missense	Damaging	29.5	37.3
FER	NM_005246	p.Tyr634Cys	g.chr5:108382876	A->G	Missense	Damaging	1.4	30.4
FNDC1	NM_032532	p.Arg189Cys	g.chr6:159636081	C->T	Missense	Damaging	29.3	35.9
OR8U1	NM_001005204	p.Asn175Ile	g.chr11:56143623	A->T	Missense	Damaging	30.0	34.1
PIDD	NM_145886	p.Arg342Cys	g.chr11:802347	C->T	Missense	Damaging	3.3	28.3
ZNF614	NM_025040	p.Glu202Gly	g.chr19:52520246	A->G	Missense	Damaging	28.7	33.7

AML, acute myeloid leukemia; MDS, myelodysplastic syndrome; MF, myelofibrosis; SIFT, sorting intolerant from tolerant; VAF, variant allele fraction.

allowed accurate determination of their VAFs; on this basis, we could establish an inferred model of clonal evolution in terms of individual mutations in subjects 20 and 21 (Fig. 2a,b; Supplementary Fig. 6a,b). Intratumoral heterogeneity was evident at both MDS and AML phases in subject 20. According to the predicted model, a founding clone with a *CDC25C* mutation acquired additional mutations in *COL9A1*, *FAM22G* and *LPP* (group A), followed by the emergence of a *GATA2* mutation (group B), which was associated with leukaemic transformation, whereas the size of another subclone, defined by mutations in *CHEK2* and three other genes (group C), was unchanged. To validate this hierarchical model, single-cell genomic sequencing was performed using genomic DNA of 63 bone marrow cells from subject 20 when the patient was in the AML phase. Assuming that all cells harbour the *RUNX1* mutation, the false-negative rate of the procedure reached 35%, possibly due to biased allele amplification (Online Methods). However, this technique successfully demonstrated that the group A/B and group C mutations were mutually exclusive (Fig. 2c; Supplementary Table 2). To statistically evaluate this possibility, we assumed two hypotheses (H_0: the mutational status of genes in group A/B and group C is independent; H_1: mutations in group A/B and group C are mutually exclusive) and calculated each probability distribution (P_i: probability that the current results as shown in Fig. 2c were obtained under the hypothesis H_i). Our mutational profile data were achieved with a much higher likelihood under H_1 than H_0 (Supplementary Fig. 7 and detailed in Supplementary Methods). Similarly, the clonal architecture for subject 21 was portrayed in Fig. 2b and Supplementary Fig. 6b. In both scenarios, *CDC25C* mutations seemed to represent a founding mutation with the highest VAF, suggesting that the *CDC25C* mutation contributed to the establishment of a founding tumour population as an early genetic event, whereas progression to AML seemed to be accompanied by the appearance of additional mutations, indicating a multistep process in leukemogenesis.

Along with the somatic mutations found in subjects 20 and 21, a *GATA2* mutation was also identified in subject 22 (Fig. 3a). This patient developed AML with multilineage dysplasia, which led to the diagnosis of AML – MRC (myelodysplasia-related changes). Remission-induction therapies were only partially effective and the blast cell count was reduced from 54 to 5.6%, while dysplastic features persisted (Fig. 3b; Supplementary Fig. 8). Allogeneic stem cell transplantation was successfully performed from a human leukocyte antigen-matched unrelated donor and durable complete remission, with 100% donor chimerism, was achieved. During treatment, the VAF of the *GATA2* mutation decreased virtually in parallel with the blast cell percentage, while the VAF of the *CDC25C* mutation hovered at a high level before transplantation. Thus, we hypothesized that the *GATA2* mutation induced leukaemia progression in this patient, whereas the *CDC25C* mutation was associated with the pre-leukaemic status. Another *GATA2* mutation (p.Leu359Val) was found in subject 18, with a VAF (0.94%), who showed only thrombocytopenia without any signs of leukaemia progression and who had a small subclone with a concurrent *CDC25C* mutation (Fig. 3c). Although *GATA2* mutations are detected in a small number of patients with FPD/AML, the findings described above suggest that mutation of *GATA2* is a key factor promoting disease progression in FPD/AML (Fig. 3d).

Biological consequences of *CDC25C* mutations. We next investigated the possible impact of *CDC25C* mutation on clonal selection and evolution. CDC25C is a phosphatase that prevents premature mitosis in response to DNA damage at the G2/M checkpoint, while it is constitutively phosphorylated at Ser216 throughout interphase by c-TAK1 (refs 8–10). When phosphorylated at Ser216, CDC25C binds to 14-3-3 protein[11], leading to sequestration of CDC25C to the cytoplasm and its inactivation. Ba/F3 cells were transduced with retroviruses encoding the wild-type or mutant CDC25C containing each of the individual mutations (p.Asp234Gly, p.Ala344Val, p.His437Asn and p.Ser216Ala), and assayed for the phosphorylation status, 14-3-3 protein-binding capacity and intracellular localization of each of these proteins. The Ser216Ala mutant form

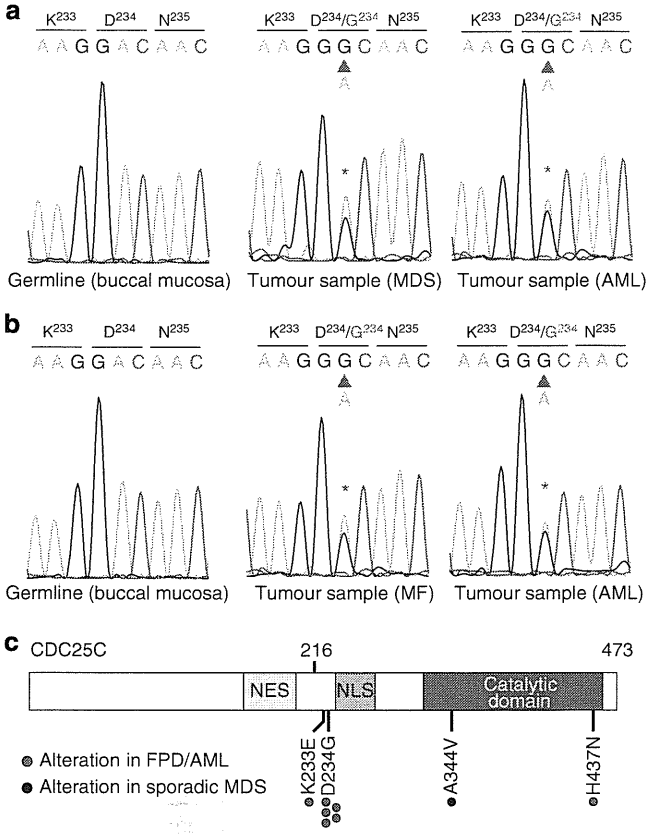

Figure 1 | Mutation in *CDC25C* recurs in cases of FPD/AML. (**a**,**b**) Sanger sequencing of *CDC25C* mutations found in whole-exome sequencing is shown. Both forward and reverse traces were available for each mutation, but only one trace is shown above. The results of buccal mucosa, pre-leukaemic phase and leukaemic phase is demonstrated for subject 20 (**a**) and subject 21 (**b**), respectively. (**c**) The distribution of alterations is shown for the CDC25C protein. NES, a putative nuclear export signal domain between amino acids 177–200; NLS, a putative nuclear localization sequence domain consisting of amino acids 240–244.

of CDC25C, which lacks the phosphorylation site, was used as a negative control. In all of the mutated forms of CDC25C, the capacity for binding to c-TAK1 was reduced (Fig. 4a,b; Supplementary Fig. 9a,b), resulting in decreased phosphorylation of CDC25C at Ser216 (Fig. 4c). Consequently, the mutant proteins failed to bind 14-3-3 protein efficiently (Fig. 4d,e; Supplementary Fig. 8c,d) and remained in the nucleus even during interphase (Fig. 4f; Supplementary Figs 10 and 11). In accordance with these observations, CDC25C mutants enhanced mitotic entry, which was exaggerated by low-dose radiation-induced DNA damage (Fig. 4g,h; Supplementary Fig. 12; Supplementary Methods). These results suggest that mutation of *CDC25C* results in disruption of the DNA checkpoint machinery. Next, we investigated why mutation of *CDC25C* is a frequent genetic event in FPD/AML. It is known that *RUNX1* mutations suppress DNA damage repair and subsequent cell cycle arrest in hematopoietic cells by means of transcriptional suppression of several genes that are involved in DNA repair[12,13]. We confirmed that FPD/AML-associated *RUNX1* mutations have similar effects, as we observed activation of the G2/M checkpoint mechanism in the presence of *RUNX1* mutations (Fig. 4i; Supplementary Fig. 13a,b). We found, however, that introduction of mutations in *CDC25C* resulted in enhanced mitosis entry, despite co-existence of *RUNX1* mutations (Fig. 4i). Therefore, we speculated that compromised DNA damage checkpoint mechanisms caused by mutations in *CDC25C* may contribute to malignant transformation, in concert with increased genomic instability due to *RUNX1* mutations.

Discussion

Whole-exome sequencing, followed by targeted deep sequencing, identified novel aspects of the pathogenesis of malignant transformation in FPD/AML. First, the high frequency of *CDC25C* mutations in FPD/AML underscores their major role in the development of haematological malignancies in FPD/AML patients. To our knowledge, *CDC25C* mutations have not been reported previously and represent a new recurrent mutational target in haematological malignancies, although *CDC25C* mutations have been reported in some solid carcinomas with unknown significance[14,15]. Furthermore, our functional assays support their biological significance, which is characterized by cell cycle progression and premature mitotic entry. Although the 5q31 minimally deleted region, in which CDC25C is located, is frequently detected in MDS, it seems to be associated with other oncogenic mechanisms since our functional assays suggested that *CDC25C* mutations in FPD/AML were gain-of-function type mutations that facilitate the mitotic entry by aberrant accumulation in the nucleus. Impaired DNA repair function mediated by germline *RUNX1* mutation may play a role in the generation of *CDC25C* mutations.

Evaluation of the allelic burden of mutated genes demonstrated that *CDC25* mutations are found with high VAFs in FPD/AML-derived leukaemia and with low VAFs in cases of thrombocytopenia. Our hierarchical model and clonal selection highlighted that mutation of *CDC25C* defines an initial event during malignant transformation and predates subclonal mutations in *GATA2* and other genes. On the basis of the observation that four of the seven FPD/AML patients with *CDC25C* mutations have developed leukaemia and that *CDC25C* mutations were actually detected in the leukaemic subclones, we speculated that a FPD/AML patient with a *CDC25C* mutation, but without clinically evident leukaemia, is at high risk for the onset of leukaemic progression. Examination of the allelic burden of *CDC25C* mutation may thus serve to evaluate the risk of leukaemic progression in patients with FPD/AML.

Among the mutations found in FPD/AML, mutations in *GATA2* were identified in 3 of 13 individuals (subjects 18, 20 and 22). *GATA2* mutations were frequently identified in FPD/AML-derived leukaemia (2/7) and in a patient with thrombocytopenia who had a small subclone bearing a *CDC25C* mutation (1/6). Although reports on the clinical relevance of *GATA2* mutations in myeloid malignancy are limited, several lines of evidence in this respect have recently been reported. *GATA2* mutations are frequently found in a subgroup of patients with cytogenetically normal AML with biallelic *CEBPA* gene mutations[16], which account for ~4% of AML. Germline *GATA2* mutations are also observed in disorders linked to an increased propensity for the development of MDS and AML, including Emberger syndrome, MonoMAC syndrome and dendritic cells, monocytes, B and natural killer cells deficiency[17–20]. The alterations in *GATA2* (leading to p.Leu321His and p.Leu359Val), which were found in FPD/AML patients in this study, are located in the part of the gene encoding the N-terminal and C-terminal zinc-finger domains, respectively (Fig. 3d). Mutations affecting the identical amino acids have been reported in AML patients bearing *CEBPA* mutations and chronic myeloid leukaemia patients in blast crisis[16,21]. Thus, *GATA2* mutation may contribute to AML progression in collaboration with *RUNX1* and/or *CDC25C* mutations. Furthermore, although

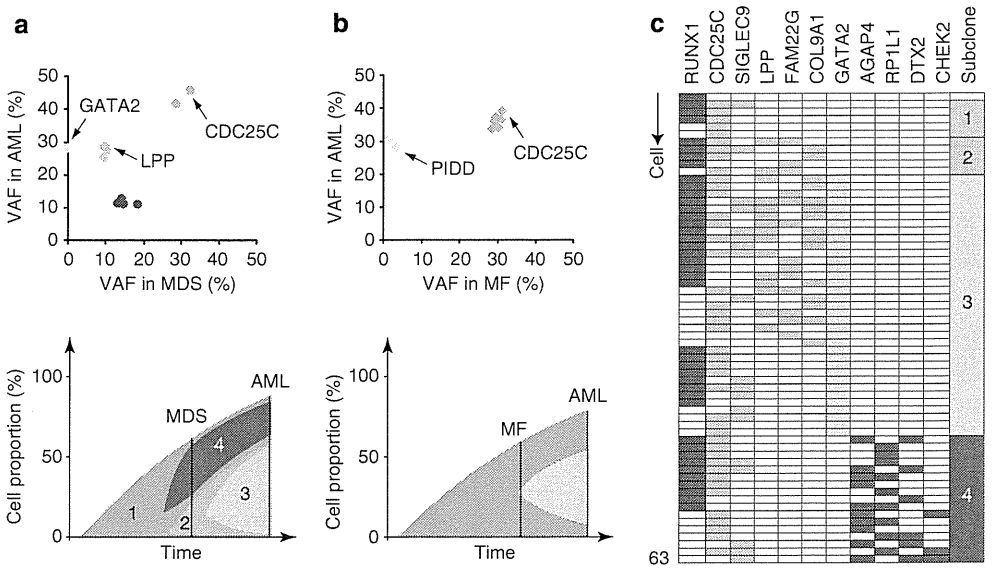

Figure 2 | Clonal evolution of FPD/AML-related myeloid disorders. (**a**,**b**) Observed variant allele fraction (VAF) of validated mutations are listed in Table 2, in both pre-leukaemic and leukaemic phases, are shown in diagonal plots (top) for subject 20 (**a**) and subject 21 (**b**). Predicted chronological behaviours in different leukemia subclones are depicted below each diagonal plot. Distinct mutation clusters are displayed by colour. The vertical axis represents cell proportion of each clone calculated by VAF × 2 (%) (because all the mutations were heterozygous), regarding the whole bone marrow as 100%. (**c**) Mutation status of each bone marrow cell from subject 20 during the acute myeloid leukemia (AML) phase. The vertical axis represents each cell ($n = 63$) and the horizontal axis displays each gene mutation. Coloured columns show that the corresponding cell harbours gene mutation(s) as defined in Online Methods. Subclone numbers shown in the right row correspond to the numbers in the lower figure of **a**.

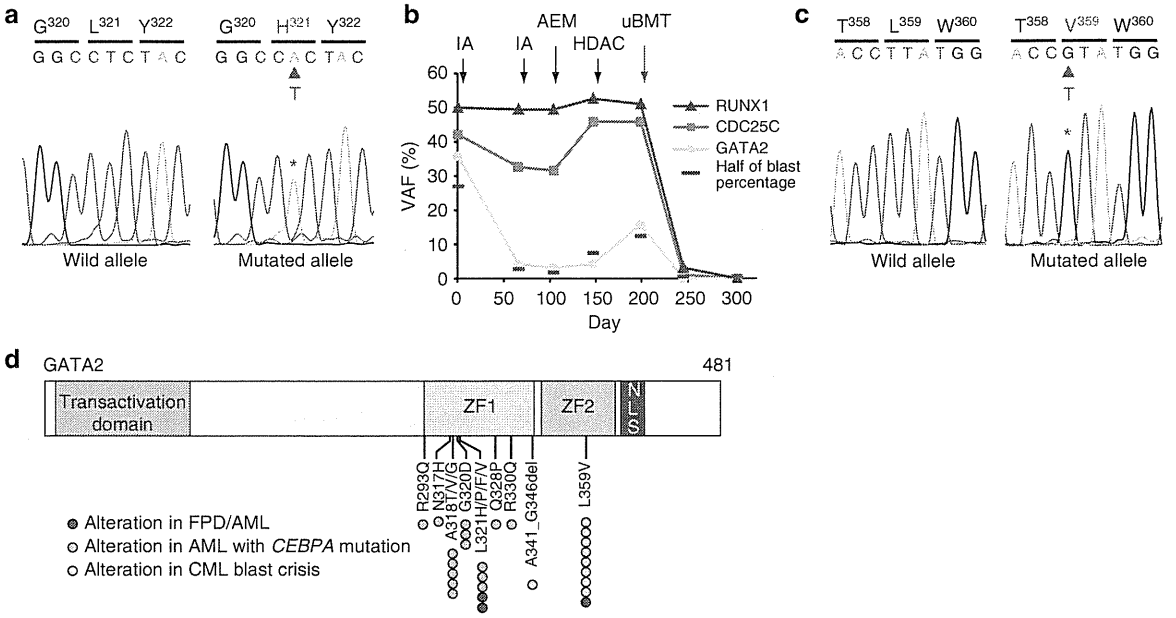

Figure 3 | *GATA2* mutations in FPD/AML. The result of Sanger sequencing for *GATA2* p.Leu321His mutation in subject 22 (**a**) and Leu359Val mutation in subject 18 (**c**) validated with subcloning strategy by methods shown in Supplementary Methods. (**b**) Variant allele fractions (VAFs) of *RUNX1*, *CDC25C* and *GATA2* mutation in subject 22 are demonstrated with the time course of treatment. Half the value of the blast cell percentage, which corresponds to the allele frequency of a heterozygous mutation, is also shown by a red bar. IA, idarubicine + Ara-C; AEM, Ara-C + etoposide + mitoxantrone; HDAC, high-dose Ara-C; uBMT, unrelated bone marrow transplantation. (**d**) Schematic representation of *GATA2* mutations. *GATA2* mutations that were identified in FPD/AML are displayed together with mutations found in AML with *CEBPA* mutation[16] as well as in CML patients in blast crisis[21]. ZF, zinc-finger domain; NLS, a putative nuclear localization sequence domain.

another report identified somatic *CBL* mutation with acquired 11q uniparental disomy as a second hit as being responsible for leukaemic transformation in FPD/AML[22], *CBL* mutations were not detected in our series of FPD/AML samples.

Although the precise pathogenetic roles of *CDC25C* mutations remain unclear, we presume that mutant CDC25C alleles confer a proliferative advantage under certain circumstances in which DNA repair machinery is compromised, such as that mediated by

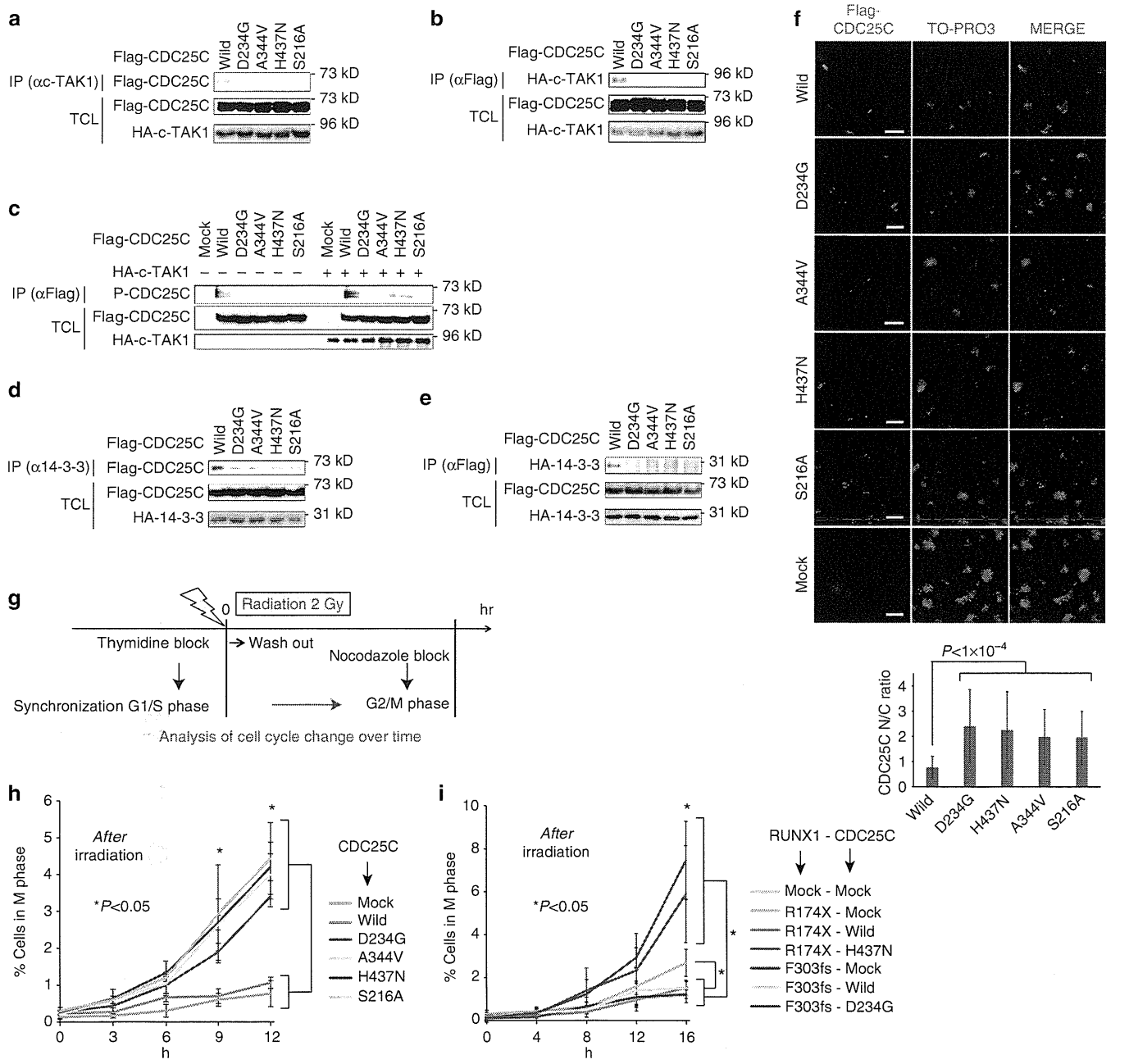

Figure 4 | Mutated CDC25C enhances mitotic entry. (**a**) HEK293T cells were transiently transfected with constructs encoding Flag-tagged CDC25C wild type or mutants, as indicated, and cell lysates were immunoprecipitated with anti-c-TAK1 antibody. Binding capacity of CDC25C was evaluated by western blotting. IP, immunoprecipitation; TCL, total cell lysate. (**b**) Reciprocal immunoprecipitation of **a** using anti-Flag (CDC25C) antibody for immunoprecipitation. (**c**) Left half; cell lysates were immunoprecipitated with anti-Flag antibody. Phosphorylation levels of CDC25C were assessed by phosphorylated-Ser216-specific anti-CDC25C antibody. Right half; the same experiment was performed with cell lysates from HEK293T cells transfected with constructs encoding Flag-tagged CDC25C wild type or mutants and HA-tagged c-TAK1. (**d**) Mutated CDC25C showed reduced capacity for binding to 14-3-3. Cell lysates were immunoprecipitated with anti-14-3-3 antibody and binding capacity of CDC25C was evaluated. (**e**) Reciprocal immunoprecipitation of **d** using anti-Flag (CDC25C) antibody for immunoprecipitation. (**f**) Localization of CDC25C or its mutants was visualized by immunofluorescence. Anti-Flag antibody and Alexa Fluor 555 antibody was used for visualization of CDC25C. N/C ratio of each cell was calculated as detailed in Supplementary Methods and Supplementary Fig. 10. The mean and s.d. of the N/C ratio is presented. Statistical significance of difference was determined by unpaired Student's *t*-test ($n>30$ for each). Scale bar, 10 μm. (**g**) Schematic description of the method used for evaluation of mitotic entry. (**h**) Mitotic entry of CDC25C-mutated cells. Percentage of mutated CDC25C-transduced cells in the M phase was compared with that of wild-type CDC25C-transduced cells. *P* values were calculated using Student's *t*-test and the differences between groups, as indicated, were all statistically significant ($^*P<0.05$) at 10 and 12 h after irradiation ($n=3$). The average and s.d. is presented. (**i**) Mutated RUNX1 and CDC25C were co-expressed in Ba/F3 cells, as indicated, and mitosis entry of these cells was evaluated. The differences between groups, as indicated, were all statistically significant ($^*P<0.05$ at 16 h after washout of thymidine ($n=3$). *P* values were determined using the Student's *t*-test. The average and s.d. is presented.

a germline *RUNX1* mutation. In addition, as Turowski and colleagues reported that CDC25C was involved in S phase entry in addition to mitotic entry[23], release from thymidine-induced G1/S block may be affected by some unknown machinery mediated by mutated CDC25Cs, which might affect the results when we observed G2/M phase fraction of these cells. It is not clear why *CDC25C* mutations are repetitively documented in FPD/AML, but not in sporadic MDS or AML cases. One possibility is that in the presence of a *RUNX1* mutation, as an initial event, an extended period is required before an additional *CDC25C* mutation is acquired. This proposal is supported by the clinical observation that ~40% of patients with FPD/AML develop leukaemia in their 30s[5]; however, the mutational status in *CDC25C* in the reported cohort was unknown.

One of the important problems in the research of FPD/AML is that definitive diagnostic criteria have not been established yet. For this purpose, more extensive studies are required for accumulating clinical characterization, genetic information and functional examination as to whether a *RUNX1* variant in families with thrombocytopenia and/or haematological malignancy is causal[24]. We clarified tentative diagnostic criteria for FPD/AML, which was used in this study (in Methods). Regarding the three missense variants in our study (p.Ser140Asn in pedigree 54, p.Gly172Glu in pedigree 57 and p.Leu445Pro in pedigree 32), Ser140 and Gly172 have been reported to be mutated in sporadic AML and/or MDS cases[25,26]. In addition, induced pluripotent stem cells from a FPD/AML pedigree with p.Gly172Glu recapitulate the phenotype of FPD/AML after hematopoietic differentiation[27]. Ser140 has been also shown to be important for RUNX1 conformation, and a mutation of this site affects hydrogen bonds and results in functional loss[28,29]. Furthermore, all the three missense variants have not been reported in the following SNP database: SNP database (dbSNP) (http://www.ncbi.nlm.nih.gov/projects/SNP), the 1000 Genomes Project (http://www.1000genomes.org), HGVB (http://www.genome.med.kyoto-u.ac.jp/SnpDB/index.html). They were also predicted as 'damaging' by Polyphen-2 (http://genetics.bwh.harvard.edu/pph2/), SIFT (http://sift.jcvi.org/) and PROVEAN (http://provean.jcvi.org/index.php). Therefore, we regarded the pedigrees with these *RUNX1* variants as having FPD/AML in this study. However, regarding pedigree 32 with p.Leu445Pro, we could not completely exclude the possibility of incidental co-occurrence of a possible non-causal *RUNX1* germline variant and hairy cell leukaemia, although co-occurrence of them is supposed to be rare. In addition, we should bear in mind the somatic as well as germline LOH of *RUNX1*, which contributes to thrombocytopenia and/or leukemogenesis in FPD/AML.

In conclusion, our results indicate that FPD/AML-associated leukaemic transformation is due to stepwise acquisition of mutations and clonal selection, which is initiated by a *CDC25C* mutation in the pre-leukaemic phase, and is further driven by mutations in other genes including *GATA2* (Supplementary Fig. 14). The identification of *CDC25C* as the target gene responsible for the leukaemic transformation will facilitate diagnosis and monitoring of individuals with FPD/AML, who are at an increased risk of developing life-threatening haematological malignancy.

Methods

Subjects. Studies involving human subjects were done in accordance with the ethical guidelines for biomedical research involving human subjects, which was developed by the Ministry of Health, Labour and Welfare, Japan; the Ministry of Education, Culture, Sports, Science, and Technology, Japan; and the Ministry of Economy, Trade, and Industry, Japan, and enforced on 29 March 2001. This study was approved by ethical committee of the University of Tokyo and each participating institution. Written informed consent was obtained from all patients whose samples were collected after the guideline was enforced. All animal experiments were approved by the University of Tokyo Ethics Committee for Animal Experiments. The clinical data, peripheral blood sample and buccal mucosa of the patients whose pedigree contained two or more individuals with thrombocytopenia and/or any haematological malignancies were collected from participating institutions. Platelet threshold depended on each institution's judge and any haematological malignancies were allowed. The diagnoses were self-reported. When all the following four criteria were fulfilled, the patient was considered as having FPD/AML in this study: (1) the pedigree has two or more individuals with thrombocytopenia and/or any haematological malignancies; (2) a germline *RUNX1* variant, including missense, nonsense, frameshift, insertion and deletion, is confirmed by Sanger sequencing and a synchronized quantitative-PCR method in at least one family member; (3) the *RUNX1* variant has not been reported in public dbSNP; (4) no germline mutations were detected in the following 16 genes: *GATA2*, *GATA1*, *CEBPA*, *MPL*, *MYH9*, *MYL9*, *GP1BA*, *GP9*, *MASTL*, *HOXA11*, *CBL*, *DIDO1*, *TERT*, *ANKRD26*, *GFI1B* and *SRP72*. Regarding the last criterion, 16 genes were selected because they have been reported to be responsible for familial thrombocytopenia and/or haematological malignancies.

Whole-exome sequencing. Genomic DNA was extracted from samples using the QIAamp DNA Mini kit (Qiagen). Exome capture was performed. Enriched exome fragments were subjected to sequencing using HiSeq2000 (Illumina). We removed any potential somatic mutations that were observed in dbSNP (http://www.ncbi.nlm.nih.gov/projects/SNP) or in the 1000 Genomes Project (http://www.1000genomes.org) data. All candidate single-nucleotide variations and indels, which were predicted to be deleterious by the Polyphen-2 algorithm, were validated by deep sequencing and Sanger sequencing. Genomic DNA samples from the buccal mucosa of the two patients (subject 20 and subject 21) were used as references. All candidate somatic mutations were validated by Sanger sequence and deep sequencing using primers listed in Supplementary Tables 3 and 4.

Deep sequencing. Using genomic DNA of the patients as template, each targeted region was PCR amplified with specific primers (Supplementary Table 4). The amplification products from an individual sample were combined and purified with the AMpure XP Kit (Beckman Coulter) and library preparation was carried out using the Ion Xpress Fragment Library Kit (Life Technologies) according to the manufacturer's instructions. The Agilent 2100 Bioanalyzer (Agilent Technologies) and the associated High Sensitivity DNA kit (Agilent Technologies) were used to determine quality and concentration of the libraries. The amount of the library required for template preparation was calculated using the template dilution factor calculation described in the protocol. Emulsion PCR and enrichment steps were carried out using the Ion OneTouch 200 Template Kit v2 DL (Life Technologies). Sequencing was undertaken using Ion Torrent PGM and Ion 318 chips Kit v2 (Life Technologies). The Ion PGM 200 Sequencing Kit (Life Technologies) was used for sequencing reactions, following the recommended protocol. The presence of *CDC25C* and *GATA2* mutations was also validated by a subclone strategy for DNA sequence analysis.

Single-cell sequencing and genome amplification. Single cells were separated from the bone marrow of subject 20 at AML phase using FACSAria II (BD biosciences) (Supplementary Fig. 15a). Each cell was deposited into individual wells of a 96-well plate. Single cells were lysed and whole genome from single cell was amplified using GenomePlex Single Cell Whole-Genome Amplification Kit (Sigma-Aldrich). Mutation status of each gene was analysed by direct sequencing with specific primers (Supplementary Table 5). To improve the sensitivity of this procedure, we used multiple primer sets for detecting a single-nucleotide variation. We estimated the false-negative rate of this procedure based on the ratio of RUNX1 mutation, which is supposed to be observed in all of the cells. The false-negative rate was estimated to be 35% (22 cells out of 63 cells, Supplementary Table 2), which is consistent with the manufacturer's bulletin reporting the allelic dropout of 30%. In light of these results, we regard those cells with at least one gene mutation in a mutational group (coloured in red, orange, green, blue or purple) as being positive for gene mutations of the corresponding group. To assess whether mutations in *LPP*, *FAM22G*, *COL9A1* and *GATA2* and mutations in *AGAP4*, *RP1L1*, *DTX2* and *CHEK2* were mutually exclusive, we performed a statistical analysis as follows. First of all, we determine a matrix **A** that virtually represents the mutational status of eight genes (1: *LPP*, 2: *FAM22G*, 3: *COL9A1*, 4: *GATA2*, 5: *AGAP4*, 6: *RP1L1*, 7: *DTX2* and 8: *CHEK2*) of 57 cells. Concretely, **A** is defined as follows:

$$\mathbf{A}=\begin{pmatrix} a_{1,1} & \cdots & a_{8,1} \\ \vdots & \ddots & \vdots \\ a_{1,57} & \cdots & a_{8,57} \end{pmatrix} \quad a_{i,j}=\begin{cases} 0: \text{if gene i of cell j is wildtype} \\ 1: \text{if gene i of cell j is mutated} \end{cases} \qquad (1)$$

On the other hand, a matrix **R** indicates data from the actual experimental results of mutational analysis as shown in Fig. 2c. Elements of **R** is provided in

Supplementary Table 2.

$$\mathbf{R}=\begin{pmatrix} r_{1,1} & \cdots & r_{8,1} \\ \vdots & \ddots & \vdots \\ r_{1,57} & \cdots & r_{8,57} \end{pmatrix} \quad r_{i,j}=\begin{cases} 0: \text{if gene i of cell j is wild type} \\ 1: \text{if gene i of cell j is mutated} \\ 2: \text{if mutational status of gene i of cell j is undetermined} \end{cases} \tag{2}$$

Then we assumed two hypotheses: H_0 and H_1.

H_0: the mutational status of genes $1\sim4$ and genes $5\sim8$ is independent. Each matrix elements of $\mathbf{A}$ are randomly assigned 0 or 1 (at ratio of 1:1) independently of each other.

H_1: mutations in genes $1\sim4$ and genes $5\sim8$ are mutually exclusive, and cells $1\sim40$ harbour mutations of genes $1\sim4$, while cells $41\sim57$ harbour mutations of genes $5\sim8$. In mathematical representation,

$$a_{i,j}=\begin{cases} 0: (5\le i\le 8 \text{ and } 1\le j\le 40) \text{ and } (1\le i\le 4 \text{ and } 41\le j\le 57) \\ 0 \text{ or } 1 \text{ randomely}: (1\le i\le 4 \text{ and } 1\le j\le 40) \text{ and } (5\le i\le 8 \text{ and } 41\le j\le 57) \end{cases} \tag{3}$$

We assumed matrices $\mathbf{A}_0$ and $\mathbf{A}_1$ that represent virtually generated mutational status under the hypotheses H_0 and H_1, and calculate the probability of substantializing $\mathbf{R}$ for given $\mathbf{A}_0$ and $\mathbf{A}_1$.

$P_0(\mathbf{R}/\mathbf{A}_0)$ and $P_1(\mathbf{R}/\mathbf{A}_1)$ can be calculated for given matrices $\mathbf{A}_0$ and $\mathbf{A}_1$ under the condition as follows:

Probability that we cannot determine whether a cell has mutation in gene X when the cell does not actually have a mutation; 28% (based on our data shown in Supplementary Table 2).

Probability that we judge that a cell has a mutation in gene X when the cell does not actually have a mutation; 5% (because it is very unlikely to happen).

Probability that we can judge correctly that a cell does not have a mutation in gene X when the cell does not actually have a mutation; 67% ($100-28-5=67\%$).

Probability that we cannot determine whether a cell has mutation in gene X when the cell actually has a mutation; 28% (based on our data shown in Supplementary Table 2).

Probability that we judge that a cell has a mutation in gene X when the cell actually has a mutation; 35% (the estimated false-negative rate based on the ratio of *RUNX1* mutation).

Probability that we can judge correctly that a cell has a mutation in gene X when the cell actually has a mutation; 37% ($100-28-35=37\%$).

Put it simply, $\mathbf{P}_0$ represents the probability that one can get the mutational profile R when a cell harbours mutations independently of each other, while $\mathbf{P}_1$ indicates the probability that R is realized under the condition where mutations in gene groups $1\sim4$ and $5\sim8$ are exclusive. Because $\mathbf{A}_0$ and $\mathbf{A}_1$ that meet the hypotheses H_0 and H_1 can be generated innumerably, we conducted a computational simulation to acquire the distribution of P_0 and P_1 by generating $\mathbf{A}_0$ and $\mathbf{A}_1$ 100,000 times. For visibility, horizontal axis is converted to $-\ln(P)$.

Synchronized quantitative-PCR. These experiments were performed mostly as described previously[6]. Briefly, genomic DNA was denatured 95 °C for 5 min and iced immediately. Using the LightCycler 480 Instrument II (Roche), thermal cycling was performed with denatured genomic DNA, forward and reverse primers (Supplementary Table 6), THUNDERBIRD SYBR qPCR mix (TOYOBO). Threshold cycle scores were determined as the average of triplicate samples. We designed 27 primers for *RUNX1* and 3 reproducible primers (that is, primer RUNX-9, RUNX-19 and RUNX-20) were chosen by preparatory experiments. RPL5-2 and PRS7-1 primers, which were authorized previously[6], were also utilized as controls. In addition, genomic DNA extracted from the bone marrow sample of a MDS patient with a chromosome 21 deletion was also examined with the same primers as a control of *RUNX1* locus copy-number loss. Crossing points (Cps) of designed primers were examined by quantitative PCR. *RUNX1* locus copy-number relative to RPL5-2 was calculated using Cps of RUNX-9 and RPL5-2, with RPL5-2 values set at 2. Similar results were obtained when Cps of RUNX-19, RUNX-20 or RPS7-1 values were used.

LOH detection with SNP sequencing. To examine the existence of uniparental disomy, we designed four specific primers to detect nine SNPs in *RUNX1*, which are frequently seen (>40%) (Supplementary Table 7). Direct sequencing was performed with the primers, and heterogeneity of SNPs was examined.

Chemicals and immunological reagents. Thymidine and nocodazole were purchased from Sigma-Aldrich. Anti-CDC25C, anti-phospho-CDC25C (Ser216) and anti-beta-actin antibodies were purchased from Cell Signaling Technology. Anti-HA monoclonal antibody was purchased from MBL. Rabbit anti-Flag monoclonal antibody was purchased from Sigma-Aldrich. Anti-HA was purchased from Roche. Mouse anti-phospho-histone H2AX (Ser139) antibody and Alexa Fluor 488 mouse anti-phospho-H3 (Ser10) antibody were purchased from Merck Millipore. Alexa Fluor 488 rabbit anti-mouse immunoglobulin (Ig)G, Alexa Fluor 488 goat anti-rabbit IgG and Alexa Fluor 555 goat anti-rabbit IgG were purchased from Invitrogen. TO-PRO3 was purchased from Molecular Probes. Rabbit anti-14-3-3 Sigma antibody was purchased from Bethyl laboratories. Sheep anti-c-TAK1 antibody was purchased from Exalpha Biologicals. Anti-sheep IgG-HRP was purchased from RSD. Nonviable cell exclusion was performed by 7-AAD Viability Staining Solution (BioLegend).

Subclone strategy and direct sequencing. Using genomic DNA of the patients as template, each targeted region was amplified by PCR with specific primers (Supplementary Table 4). PCR products were purified with illustra ExoStar (GE Healthcare) and subcloned into *Eco*RV site of pBluescript II KS(−) (Stratagene). Ligated plasmids were transformed into *E. coli* strain XL1-Blue by 45 s heat shock at 42 °C. Positive transformants were incubated on LB plates containing 100 μg ml^{-1} ampicillin supplemented with X-gal (Sigma-Aldrich) and isopropyl β-D-1-thiogalactopyranoside (Sigma-Aldrich). For colony PCR, a portion of a white colony was directly added to a PCR mixture as the DNA template. Insert region was amplified by PCR procedure with T3 and T7 universal primers, purified with illustra ExoStar (GE Healthcare Life Sciences), and sequenced by the Sanger method with T3 and T7 primers using BigDye Terminator v3.1 Cycle Sequencing kit (Applied Biosystems) and ABI Prism 310 Genetic Analyzer (Life Technologies).

Immunoprecipitation and western blotting. These experiments were performed as described previously[30]. Briefly, HEK293T cells were transiently transfected with mammalian expression plasmids encoding Flag-tagged CDC25C and its mutants, HA-tagged 14-3-3 or c-TAK1. All plasmids were sequence verified. After 48 h, cell lysates were collected and incubated with an antibody (anti-HA antibody (1:200, 3 h), anti-Flag antibody (1:200, 3 h), anti-c-TAK1 antibody (1:150, 3 h) and anti 14-3-3 antibody (1:150, 3 h)). After incubation, the cell lysates were incubated with protein G-Sepharose (GE Healthcare) for 1 h. The precipitates were stringently washed with high salt-containing wash buffer and analysed by western blotting. Anti-Flag (HRP-conjugated, Sigma-Aldrich), anti-HA (MBL), anti-HA (HRP-conjugated, Roche), anti-CDC25C (Cell Signaling Technology), anti-phospho-CDC25C (Ser216) (Cell Signaling Technology), anti-c-TAK1 antibody (Exalpha Biologicals) or anti-14-3-3 antibody (Bethyl laboratories) antibodies and Immunostar LD (Wako) was used for detection. Original gel images of western blot analysis are shown in Supplementary Fig. 16.

Cell cycle synchronization and analysis for mitosis entry. After transduction of wild-type CDC25C or its mutated forms to murine lymphoid cell line Ba/F3 cells (RIKEN BioResource Center), double-thymidine block was performed to obtain cell cycle synchronization at G1/S phase. In brief, 2 mM of thymidine was added to the medium. After 16 h, cells were washed and released from the first thymidine for 8 h. A second block was initiated by adding 2 mM of thymidine, and cells were maintained for 16 h. Then thymidine was washed out and the cells were incubated with 1 mM nocodazole with or without 2 Gy of irradiation (Supplementary Fig. 10a). Ba/F3 cells were fixed over time with 75% ethanol in phosphate-buffered saline (PBS) at 4 °C overnight and permeabilized with 2% Triton-X at 4 °C for 15 min. The cells were stained with anti-phospho-H3 (Ser10) Alexa Fluor 488 conjugated antibody (dilution, 1:200) in PBS with 2% fetal calf serum at 4 °C for 30 min and then treated with 5% propidium iodide and 1% RNase in PBS at room temperature (RT) for 30 min. Cell cycle was analysed using a BD LSR II Flow cytometer (BD biosciences) (Supplementary Fig. 15b). To assess the cooperation of *CDC25C* and *RUNX1* mutation, wild-type or mutant (D234G, H437N) pMXs-neo-Flag-CDC25C and mutant (F303fsX566, R174X) pGCDNsam-IRES-KusabiraOrange-Flag-RUNX1 were retrovirally transduced into Ba/F3 cells.

Immunofluorescent microscopic analysis. These experiments were performed as described previously[30]. Briefly, Ba/F3 cells were fixed, permeabilized and blocked. Staining for phosphorylated histone H2AX was performed with anti-phospho-histone H2AX (Ser139) antibody (dilution, 1:500; Merck Millipore) at RT for 3 h. After washing with PBS three times and with 1% bovine serum albumin in PBS, the cells were treated with Alexa Fluor 488 rabbit anti-mouse IgG (dilution, 1:500; Invitrogen) and TO-PRO3 (dilution, 1:1,000; Molecular Probes) for 1 h. The proteins were visualized using FV10i (Olympus) or BZ-9000 (Keyence). The percentage of γH2AX foci-positive cells was determined by examining 100 cells per sample. Three independent experiments were performed. To evaluate the localization of CDC25C, Ba/F3 cells were treated with 2 mM thymidine for 12 h and stained. Staining was underwent with anti-Flag antibody or anti-CDC25C antibody at RT for 3 h. After washing, the cells were treated with Alexa Fluor 488 or 555 antibody and TO-PRO3 for 1 h. The mean intensity of CDC25C in the nucleus and cytoplasm of each cell was measured within a region of interest placed within the nucleus and cytoplasm (Supplementary Fig. 10). Similarly, the background intensity was quantified within the region of interest placed outside the cells. All the measurements were performed using the Fluoview FV10i software or ImageJ. The background-subtracted intensity ratio of the nucleus to cytoplasm was calculated in >30 cells in each specimen.

Retrovirus production. The procedures were performed as described previously[30]. Briefly, Plat-E packaging cells were transiently transfected with each retroviral construct using the calcium phosphate precipitation method, and supernatant

containing retrovirus was collected 48 h after transfection and used for infection after it was centrifuged overnight at 10,000 r.p.m.

Statistical analysis. To compare data between groups, unpaired Student's *t*-test was used when equal variance were met by the *F*-test. When unequal variances were detected, the Welch *t*-test was used. Differences were considered statistically significant at a P value of <0.05.

References

1. Song, W. J. *et al.* Haploinsufficiency of CBFA2 causes familial thrombocytopenia with propensity to develop acute myelogenous leukaemia. *Nat. Genet.* **23,** 166–175 (1999).
2. Ichikawa, M. *et al.* A role for RUNX1 in hematopoiesis and myeloid leukemia. *Int. J. Hematol.* **97,** 726–734 (2013).
3. Cameron, E. R. & Neil, J. C. The Runx genes: lineage-specific oncogenes and tumor suppressors. *Oncogene* **23,** 4308–4314 (2004).
4. Nickels, E. M., Soodalter, J., Churpek, J. E. & Godley, L. A. Recognizing familial myeloid leukemia in adults. *Ther. Adv. Hematol.* **4,** 254–269 (2013).
5. Liew, E. & Owen, C. Familial myelodysplastic syndromes: a review of the literature. *Haematologica* **96,** 1536–1542 (2011).
6. Kuramitsu, M. *et al.* Extensive gene deletions in Japanese patients with diamond-blackfan anemia. *Blood* **119,** 2376–2384 (2012).
7. Kirito, K. *et al.* A novel RUNX1 mutation in familial platelet disorder with propensity to develop myeloid malignancies. *Haematologica* **93,** 155–156 (2008).
8. Boutros, R., Lobjois, V. & Ducommun, B. CDC25 phosphatases in cancer cells: key players? Good targets? *Nat. Rev. Cancer* **7,** 495–507 (2007).
9. Kastan, M. B. & Bartek, J. Cell-cycle checkpoints and cancer. *Nature* **432,** 316–323 (2004).
10. Peng, C. Y. *et al.* C-TAK1 protein kinase phosphorylates human Cdc25C on serine 216 and promotes 14-3-3 protein binding. *Cell Growth Differ.* **9,** 197–208 (1998).
11. Lopez-girona, A., Furnari, B., Mondesert, O. & Early, P. R. Nuclear localization of Cdc25 is regulated by DNA damage and a 14-3-3 protein. *Nature* **397,** 172–175 (1999).
12. Satoh, Y., Matsumura, I., Tanaka, H. & Harada, H. C-terminal mutation of RUNX1 attenuates the DNA-damage repair response in hematopoietic stem cells. *Leukemia* **26,** 303–311 (2011).
13. Krejci, O. *et al.* p53 signaling in response to increased DNA damage sensitizes AML1-ETO cells to stress-induced death. *Blood* **111,** 2190–2199 (2008).
14. Park, J. *et al.* Mutation profiling of mismatch repair-deficient colorectal cancers using an in silico genome scan to identify coding microsatellites advances in brief mutation profiling of mismatch repair-deficient colorectal cancers using an in silico genome scan to Ide. *Cancer Res.* **62,** 1284–1288 (2002).
15. Vassileva, V., Millar, A., Briollais, L., Chapman, W. & Bapat, B. Genes involved in DNA repair are mutational targets in endometrial cancers with microsatellite instability. *Cancer Res.* **62,** 4095–4099 (2002).
16. Greif, P. A. *et al.* GATA2 zinc finger 1 mutations associated with biallelic CEBPA mutations define a unique genetic entity of acute myeloid leukemia. *Blood* **120,** 395–403 (2012).
17. Ostergaard, P. *et al.* Mutations in GATA2 cause primary lymphedema associated with a predisposition to acute myeloid leukemia (Emberger syndrome). *Nat. Genet.* **43,** 929–931 (2011).
18. Hahn, C. N. *et al.* Heritable GATA2 mutations associated with familial myelodysplastic syndrome and acute myeloid leukemia. *Nat Genet.* **43,** 1012–1017 (2011).
19. Hsu, A. P. *et al.* Mutations in GATA2 are associated with the autosomal dominant and sporadic monocytopenia and mycobacterial infection (MonoMAC) syndrome. *Blood* **118,** 2653–2655 (2011).
20. Dickinson, R. E. *et al.* Exome sequencing identifies GATA-2 mutation as the cause of dendritic cell, monocyte, B and NK lymphoid deficiency. *Blood* **118,** 2656–2658 (2011).
21. Zhang, S.-J. *et al.* Gain-of-function mutation of GATA-2 in acute myeloid transformation of chronic myeloid leukemia. *Proc. Natl Acad. Sci. USA* **105,** 2076–2081 (2008).
22. Hasegawa, D. *et al.* CBL mutation in chronic myelomonocytic leukemia secondary to familial platelet disorder with propensity to develop acute myeloid leukemia (FPD/AML). *Blood* **119,** 2612–2614 (2012).
23. Turowski, P. *et al.* Functional cdc25C dual-specificity phosphatase is required for S-phase entry in human cells. *Mol. Biol. Cell* **14,** 2984–2998 (2003).
24. Michaud, J. *et al.* In vitro analyses of known and novel RUNX1/AML1 mutations in dominant familial platelet disorder with predisposition to acute myelogenous leukemia: Implications for mechanisms of pathogenesis. *Blood* **99,** 1364–1372 (2002).
25. Kohlmann, A. *et al.* Monitoring of residual disease by next-generation deep-sequencing of RUNX1 mutations can identify acute myeloid leukemia patients with resistant disease. *Leukemia* **28,** 129–137 (2014).
26. Chen, C. Y. *et al.* RUNX1 gene mutation in primary myelodysplastic syndrome - The mutation can be detected early at diagnosis or acquired during disease progression and is associated with poor outcome. *Br. J. Haematol.* **139,** 405–414 (2007).
27. Sakurai, M. *et al.* Impaired hematopoietic differentiation of RUNX1-mutated induced pluripotent stem cells derived from FPD/AML patients. *Leukemia.* (epub ahead of print 15 April 2014; doi:10.1038/leu.2014.136).
28. Bravo, J., Li, Z., Speck, N. A. & Warren, A. J. The leukemia-associated AML1 (Runx1)-CBF beta complex functions as a DNA-induced molecular clamp. *Nat. Struct. Biol.* **8,** 371–378 (2001).
29. Akamatsu, Y., Tsukumo, S. I., Kagoshima, H., Tsurushita, N. & Shigesada, K. A simple screening for mutant DNA binding proteins: application to murine transcription factor PEBP2?? subunit, a founding member of the Runt domain protein family. *Gene* **185,** 111–117 (1997).
30. Yoshimi, A. *et al.* Evi1 represses PTEN expression and activates PI3K/AKT/mTOR via interactions with polycomb proteins. *Blood* **117,** 3617–3628 (2011).

Acknowledgements

This work was supported in part by grants-in-aid from the Ministry of Health, Labor and Welfare of Japan (H23-Nanchi-Ippan-104; M. Kurokawa) and KAKENHI (24659457; M. Kurokawa). We thank R. Lewis (University of Nebraska Medical Center) and T. Kitamura (Institute of Medical Science, The University of Tokyo) for providing essential materials; T. Koike (Nagaoka Red Cross Hospital), K. Nara (Ootemachi Hospital), K. Suzuki (Japanese Red Cross Medical Center), H. Harada (Fujigaoka Hospital), Y. Morita (Kinki University), M. Matsuda (PL Hospital), H. Kashiwagi (Osaka University), T. Kiguchi (Chugoku Central Hospital), T. Masunari (Chugoku Central Hospital), K. Yamamoto (Yokohama City Minato Red Cross Hospital), T. Takahashi (Mitsui Memorial Hospital) and T. Takaku (Juntendo University) for providing patient samples; M. Kuramitsu (National Institutte of Infectious Diseases) for providing kind support of synchronized quantitative PCR; and K. Tanaka and Y. Shimamura for their technical assistance.

Author contributions

A.Y., T.T., M.I. and M. Kurokawa analysed genetic materials and performed functional studies. A.T., H.I., M.N., Y.N. and S.A. were involved in sequencing and/or functional studies. M. Kawazu, T.U. and H.M. took part in whole-exome sequencing, deep sequencing and bioinformatics analyses of the data. A.Y., T.T., M.I., H.H., K.U., Y.H., E.I., K.K. and H.N. collected specimens. A.Y. and T.T. generated figures and tables. M. Kurokawa designed and led the entire project. A.Y., T.T. and M. Kurokawa wrote the manuscript. All authors participated in the discussion and interpretation of the data.

Additional information

Accession codes: Sequence data for FPD/AML patients has been deposited in GenBank/EMBL/DDBJ sequence read archive (SRA) under the accession code SRP043031

Supplementary Information accompanies this paper at http://www.nature.com/naturecommunications

Competing financial interests: The authors declare no competing financial interests.

Reprints and permission information is available online at http://npg.nature.com/reprintsandpermissions

How to cite this article: Yoshimi, A. *et al.* Recurrent *CDC25C* mutations drive malignant transformation in FPD/AML. *Nat. Commun.* 5:4770 doi: 10.1038/ncomms5770 (2014).

Brief Report

PLATELETS AND THROMBOPOIESIS

ACTN1-related thrombocytopenia: identification of novel families for phenotypic characterization

Roberta Bottega,[1] Caterina Marconi,[2] Michela Faleschini,[3] Gabriele Baj,[4] Claudia Cagioni,[5] Alessandro Pecci,[5] Tommaso Pippucci,[2] Ugo Ramenghi,[6] Simonetta Pardini,[7] Loretta Ngu,[8] Carlo Baronci,[9] Shinji Kunishima,[10] Carlo L. Balduini,[5] Marco Seri,[2] Anna Savoia,[1-3] and Patrizia Noris[5]

[1]Institute for Maternal and Child Health, Istituto di Ricovero e Cura a Carattere Scientifico Burlo Garofolo, Trieste, Italy; [2]Genetica Medica, Dipartimento di Scienze Mediche Chirurgiche, Policlinico Sant'Orsola-Malpighi, University of Bologna, Bologna, Italy; [3]Department of Medical Sciences and [4]Department of Life Sciences, University of Trieste, Trieste, Italy; [5]Department of Internal Medicine, University of Pavia, Istituto di Ricovero e Cura a Carattere Scientifico Policlinico San Matteo Foundation, Pavia, Italy; [6]Hematology Unit, Pediatric Department, University of Torino, Torino, Italy; [7]Istituto di Ematologia, Azienda Ospedaliero-Universitaria di Sassari, Sassari, Italy; [8]Royal Devon & Exeter Hospital, Devon, United Kingdom; [9]Department of Pediatric Hematology and Oncology, Pediatric Hospital "Bambino Gesù", Rome, Italy; and [10]Department of Advanced Diagnosis, Clinical Research Center, National Hospital Organization Nagoya Medical Center, Nagoya, Japan

Key Points

- *ACTN1* mutations were identified in 10 of 239 families with inherited thrombocytopenia of unknown origin.
- *ACTN1*-related thrombocytopenia is characterized by mild thrombocytopenia with platelet macrocytosis and low risk for bleeding.

Inherited thrombocytopenias (ITs) are a heterogeneous group of syndromic and nonsyndromic diseases caused by mutations affecting different genes. Alterations of *ACTN1*, the gene encoding for α-actinin 1, have recently been identified in a few families as being responsible for a mild form of IT (*ACTN1*-related thrombocytopenia; *ACTN1*-RT). To better characterize this disease, we screened *ACTN1* in 128 probands and found 10 (8 novel) missense heterozygous variants in 11 families. Combining bioinformatics, segregation, and functional studies, we demonstrated that all but 1 amino acid substitution had deleterious effects. The clinical and laboratory findings of 31 affected individuals confirmed that *ACTN1*-RT is a mild macrothrombocytopenia with low risk for bleeding. Low reticulated platelet counts and only slightly increased serum thrombopoietin levels indicated that the latest phases of megakaryopoiesis were affected. Given its relatively high frequency in our cohort (4.2%), *ACTN1*-RT has to be taken into consideration in the differential diagnosis of ITs. (*Blood*. 2015;125(5):869-872)

Introduction

Inherited thrombocytopenias (ITs) are a highly heterogeneous group of diseases characterized by different degrees of severity and complexity.[1] The variable clinical phenotype derives from a wide genetic heterogeneity, with at least 22 genes having been identified so far.[2-4] Moreover, mutations in known genes account for only 50% of patients, indicating that not all the existing forms have yet been identified. One of the most recently recognized disorders is *ACTN1*-related thrombocytopenia (*ACTN1*-RT), an autosomal -dominant form caused by mutations in the gene (*ACTN1*) encoding for 1 of the 2 nonmuscle isoforms of α-actinin 1.[5] Mainly expressed in megakaryocytes and platelets,[5] *ACTN1* has a binding domain for cross-linking the actin filaments into bundles. Based on the 7 families described in the literature, *ACTN1*-RT is characterized by mild macrothrombocytopenia and bleeding tendency, and no additional defects associated with low platelet count.[5,6] To better characterize *ACTN1*-RT, we studied 10 families identified after the screening of *ACTN1* in 128 probands with an IT of unknown origin.

Research design and methods

Of 239 consecutive probands with IT examined at the Istituto di Ricovero e Cura a Carattere Scientifico Policlinico San Matteo Foundation in Pavia, Italy, we enrolled all individuals (n = 128) without a certain diagnosis after the IT diagnostic work-up.[7,8] Mutational screening of *ACTN1* was carried out by whole-exome sequencing in 7 individuals and Sanger sequencing in the remaining 121 probands, as indicated in supplemental Table 1, available on the *Blood* Web site. Pathogenetic effects of variants were investigated by segregation analysis, bioinformatic tools, and immunofluorescence studies (supplemental Table 1; Figure 1; supplemental Figure 1). Medical history (family history included), bleeding tendency, and outcome of

Submitted August 11, 2014; accepted October 17, 2014. Prepublished online as *Blood* First Edition paper, October 31, 2014; DOI 10.1182/blood-2014-08-594531.

R.B., C.M., and M.F. contributed equally to this study.

The online version of this article contains a data supplement.

There is an Inside *Blood* Commentary on this article in this issue.

The publication costs of this article were defrayed in part by page charge payment. Therefore, and solely to indicate this fact, this article is hereby marked "advertisement" in accordance with 18 USC section 1734.

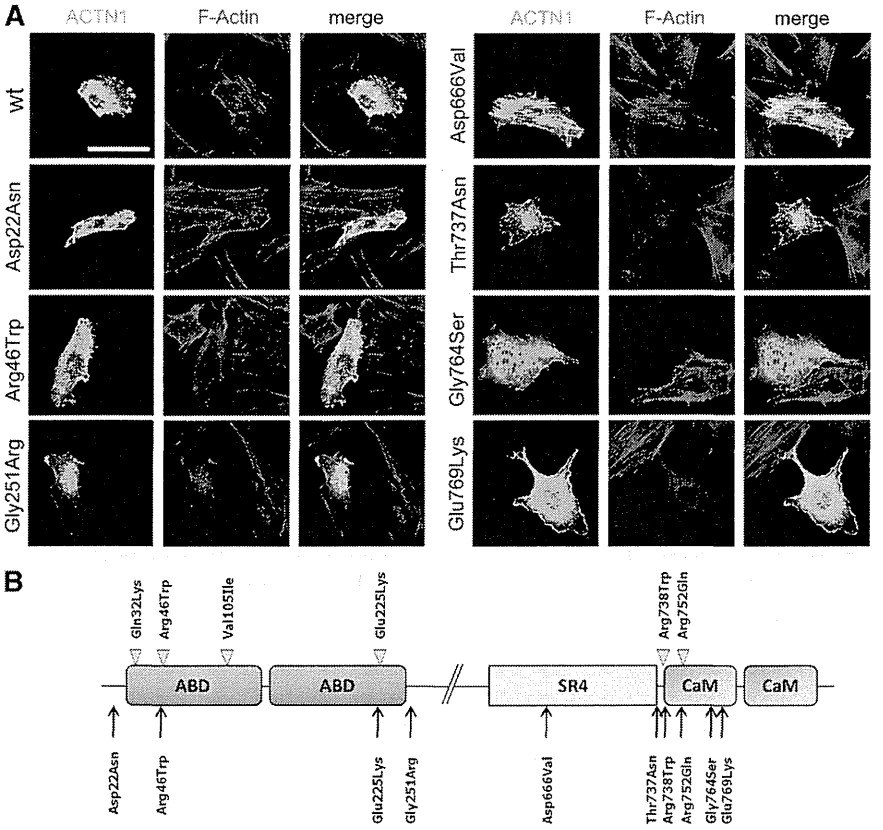

Figure 1. Functional studies of novel *ACTN1* variants. (A) Immunofluorescence analysis in PD220 fibroblast cell line transiently transfected according to standard procedures. Both wild-type (wt) or mutant *ACTN1* cDNAs were cloned into the pcDNA3.1-Myc tagged expression vector.[5] The subcellular localization of exogenous α-actinin 1 (green) was examined using c-myc antibodies (9E10; Santa Cruz Biotechnology), whereas the actin filaments were stained with AlexaFluor594 (red) conjugated phalloidin (Invitrogen). Images were obtained with a Nikon C1si confocal microscope, using ×60 Plan Apo objectives. Images were processed for z-projection (maximum intensity), brightness, and contrast regulation, using ImageJ 1.45 (National Institutes of Health). The cells shown are representative of 3 independent experiments. Scale bar = 50 μm. (B) Domain structure of α-actinin and localization of ACTN1 mutations identified in Japanese families (arrowheads)[5] and in this article (arrows). The p.Arg46Gln mutation was also identified in a French family.[6] α-actinin is organized in an actin-binding domain (ABD) at the N terminus, 4 spectrin repeats, and a calmodulin-like domain (CaM) at the C terminus. Antiparallel molecules dimerize in rod-like structures with the ABD at each extremity for cross-linking the actin filaments into bundles.

possible surgeries and pregnancies were ascertained from medical records or patient interviews. Research was conducted in accordance with the Declaration of Helsinki.

Results and discussion

Characterization of *ACTN1* missense variants

Mutational screening of *ACTN1* identified 10 different missense variants in 11 of 128 probands (supplemental Table 1). Whereas 2 (p.Arg738Trp and p.Arg752Gln) were known mutations,[5] the others were novel variants not enlisted in the Single Nucleotide Polymorphism Database. Interestingly, c.136C>T (p.Arg46Trp) was found in 2 families and affected the same residue hit by the known c.137G>A (p.Arg46Gln) mutation.[5,6] The 8 novel variants affected highly conserved amino acid residues (data not shown), and different pathogenicity prediction tools indicated deleterious effects. All but 1 (p.Asp666Val) of the variants segregated with thrombocytopenia within pedigrees when family members were available (supplemental Figure 1).

To determine the pathogenetic role of the novel missense variants, we performed immunofluorescence analysis in human fibroblasts (Figure 1A). Transfecting wild-type constructs, we observed that the cytoskeleton was organized in filaments, with ACTN1 colocalizing with actin. In cells expressing all but 1 (p.Asp666Val) of the mutations, ACTN1 was instead distributed uniformly within the cytoplasm, and actin was no longer organized in filaments. Consistent with segregation analysis, the correct organization of the cytoskeleton in cells expressing p.Asp666Val excluded this variant as a disease-causing mutation. It is worth noting that p.Asp666Val is outside the actin-binding and calmodulin-like domains (Figure 1B), suggesting that only alterations of these functional regions are compatible with the disease.

ACTN1-RT as a mild form of thrombocytopenia with slight platelet macrocytosis

Of the 10 families with pathogenetic variants, 9 were from Italy and 1 from the United Kingdom. Of the 31 affected family members, 22 were females and 9 males, indicating a potential diagnostic bias because of menorrhagia. At the time of recognition of thrombocytopenia (Table 1[9,10]), the patients' mean age was 34.5 years (range, 3-82 years). Mean platelet count was slightly reduced ($103 \pm 26 \times 10^9$/L), with only 1 patient having a platelet count lower than the cut-off value (50×10^9/L) for a safe platelet count.[11] Of note, 2 young girls (families 5 and 8) had a platelet count slightly above 150×10^9/L, but they were considered thrombocytopenic according to the age- and sex-specific reference intervals in the Italian population.[9] Both mean platelet volume (12.6 ± 1.7 fL; 95% confidence interval [CI], 12.0-13.2 fL) and diameter (3.2 ± 0.5 μm; 95% CI, 3.0-3.4 μm) were significantly higher in *ACTN1*-RT than in 50 control patients, with values of 10.1 ± 1.4 fL (95% CI, 9.7-10.4 fL) and 2.4 ± 0.3 μm (95% CI, 2.3-2.5 μm), respectively.

The mean reticulated platelet count evaluated in 9 patients using a hematology analyzer was lower ($1.16 \pm 0.64 \times 10^9$/L; 95% CI, 0.48-2.07 per liter) than in 15 control patients ($4.3 \pm 0.96 \times 10^9$/L; 95% CI, 3.55-5.24 per liter), indicating that thrombocytopenia derived from reduced platelet formation. To further investigate this aspect, we measured the serum thrombopoietin (TPO) concentration, which is inversely related to the total megakaryocyte and platelet mass,[12]

Table 1. Features of families with *ACTN1* mutations

Family (number of individuals)	Mean age at diagnosis, years (range)	World Health Organization bleeding score*	Mean platelet count,†‡ $\times 10^9$/L (range)	Mean platelet volume,† fL (range)	Mean platelet diameter,¶ μm (range)	ACTN1 mutation
F1 (4)	43 (22-55)	0 (1), 1 (3)	107 (89-134)	11.1 (10.1-12.0)	2.8 (2.7-3.0)	p.Asp22Asn
F2 (4)	46 (26-64)	0 (1), 1 (2), 2 (1)	103 (81-118)	12.5 (10.6-14.7)	3.3 (3.0-3.7)	p.Arg46Trp
F3 (4)	42 (14-72)	0 (1), 1 (1), 2 (2)	95 (66-124)	14.8 (14.0-15.6)	3.8 (3.5-4.1)	p.Arg46Trp
F4 (2)	30 (12-49)	0 (2)	103 (97-110)	11.8 [11.3-12.4)	3 (2.8-3.1)	p.Glu225Lys
F5 (6)	23 (7-44)	0 (1), 1 (3), 2 (3)	103 (78-**154**)	12.3 [10.4-14.0)	3.3 (2.6-4.3]	p.Gly251Arg
F6 (2)	58 (34-82)	2 (2)	58 (55-62)	10.5 [10.4-10.6)	3.2 (2.9-3.5]	p.Thr737Asn
F7 (1)	nd	0 (1)	110	12.1	2.5	p.Arg738Trp
F8 (3)	25 [3-44)	0 (2), 1 (1)	112 (65-**166**)	12.5 (11.3-14.3)	2.8 (2.6-3.0]	p.Arg752Gln
F9 (1)	48	0 (1)	117	14.4	3.3	p.Gly764Ser
F10 (4)	38 [3-66)	0 (1), 1 (2), 2 (1)	86 (46-120)	14-3 [12.6-15)	3.5 (2.9-3.9)	p.Glu769Lys

nd, not determined.

*World Health Organization bleeding score: grade 0, no bleeding; grade 1, only cutaneous bleeding; grade 2, mild blood loss; grade 3, gross blood loss, requiring transfusion; grade 4, debilitating blood loss, retinal or cerebral, associated with fatality.

†Platelet count and mean platelet volume were measured with a Cell-Dyn Sapphire hematology analyzer (Abbott) in EDTA-anticoagulated blood samples within 1 hour from venipuncture.

‡One individual from family 5 and 1 person from family 8 with more than 150 $\times$ 10^9 platelets/L (bold) were classified as thrombocytopenic according to the recently proposed age- and sex-specific reference intervals.[9]

¶Mean platelet diameter was measured on peripheral blood films by optical microscopy and software-assisted image analysis (Axio-vision 4.5; Carl Zeiss), as previously reported.[10] In brief, blood smears prepared with non-anticoagulated blood from fingerstick were stained with May-Grünwald-Giemsa staining, and the mean platelet diameter was calculated from 200 different cells.

with a commercially available ELISA kit (Quantikine Human TPO Immunoassay, R&D). The mean TPO level was slightly higher (22.3 ± 6.5 pg/mL; 95% CI, 13.1-31.5 pg/mL) in the 14 examined patients than in control patients (n = 40; 14.6 ± 10.8 pg/mL; 95% CI, 11.1-18.0 pg/mL), suggesting normal megakaryopoiesis, as revealed by bone marrow examination of the only patient who received this test.[6] Both young platelet count and TPO levels indicate that thrombocytopenia derives from defects of the latest phases of megakaryocyte maturation. Consistent with this conclusion, investigations in mouse megakaryocytes showed that they had defective proplatelet formation and platelet release when expressing *ACTN1* mutants.[5]

In vitro platelet aggregation in response to ADP, collagen, and ristocetin was normal, and the expression level of glycoproteins (GPs) GPIbα, GPIX, GPIIb, and GPIIIa on the platelet surface was increased, as expected in individuals with platelet macrocytosis (supplemental Table 2). Consistent with mild thrombocytopenia, as well as with platelet aggregation and expression of major platelet glycoproteins in the normal range, spontaneous bleeding tendency was absent or mild, with a few episodes of epistaxis, gum bleeding, easy bruising, and menorrhagia (Table 1). Only 3 females received iron therapy for menorrhagia. Four of the 18 patients undergoing surgery had excessive bleeding, but only 1 needed platelet transfusions. Of the 30 deliveries, only 1 had increased blood loss. Although limited, these severe hemorrhagic episodes suggest caution when hemostatic challenges occur.

Finally, we did not observe additional phenotypic defects consistently associated with *ACTN1* mutations. However, it is worth mentioning that 3 individuals from family 2, whose genotypes and platelet counts were not available, developed leukemia (both age of onset and type of leukemia were not available) (supplemental Figure 1). Moreover, individuals from families 1 and 5 had mitral valve prolapse and/or atrial septal defect (supplemental Figure 1). Because 1 individual with atrial septal defect (family 5) did not carry the mutation (p.Gly251Arg) segregating with thrombocytopenia in his family, a gene other than *ACTN1* is likely to be responsible at least for this heart malformation. Because the search for cardiac anomalies was not systematically performed in our case series, we cannot exclude that other patients with *ACTN1*-RT had similar defects. Hence, echocardiography may be appropriate in this form of IT.

ACTN1-RT is relatively common among the different forms of IT, at least in Italy and Japan.[5] Indeed, we identified *ACTN1* mutations in 10 (4.2%) of 239 consecutive IT families, a frequency similar to that reported in the Japanese population (3.7%).[5] Considering only the ITs with large platelets, the frequency is 6.6% in our population. However, we cannot exclude that *ACTN1*-RT is more frequent than expected, as affected subjects have no pathognomonic features and may be easily misdiagnosed as having immune thrombocytopenia.[13] Four of our patients had this diagnosis, and 3 were treated with steroids without any effect on platelet count. Therefore, molecular genetic testing, combined with segregation analysis and functional assays carried out to discriminate between pathogenic and silent variants, is the only diagnostic approach to identify patients with *ACTN1*-RT.

Acknowledgments

We thank Professor Kerry J. Rhoden for his critical review of the manuscript.

This work was supported by grants GGP13082 from Telethon Foundation (P.N., A.S.) and 15/12 and 16/12 (Ricerca Corrente) from Istituto di Ricovero e Cura a Carattere Scientifico Burlo Garofolo (A.S.).

Authorship

Contribution: R.B., C.M., and T.P. carried out mutational screening and analyzed data; M.F. and G.B. performed immunofluorescence analysis and analyzed data; S.K. generated vectors; A.P., C.C., U.R., S.P., L.N., C.B., and P.N. enrolled patients, provided biological samples and analyzed clinical data; and C.L.B., M.S., A.S., and P.N. designed research, interpreted data, and wrote the manuscript.

Conflict-of-interest disclosure: The authors declare no competing financial interests.

Correspondence: Anna Savoia, Department of Medical Sciences, University of Trieste, IRCCS Burlo Garofolo, Via dell'Istria 65/1, 34137 Trieste; e-mail: anna.savoia@burlo.trieste.it.

References

1. Balduini CL, Savoia A. Genetics of familial forms of thrombocytopenia. *Hum Genet.* 2012;131(12): 1821-1832.
2. Kunishima S, Saito H. Congenital macrothrombocytopenias. *Blood Rev.* 2006;20(2): 111-121.
3. Nurden AT, Freson K, Seligsohn U. Inherited platelet disorders. *Haemophilia.* 2012;18(Suppl 4): 154-160.
4. Manchev VT, Hilpert M, Berrou E, et al. A new form of macrothrombocytopenia induced by a germ-line mutation in the PRKACG gene. *Blood.* 2014;124(16):2554-2563.
5. Kunishima S, Okuno Y, Yoshida K, et al. ACTN1 mutations cause congenital macrothrombocytopenia. *Am J Hum Genet.* 2013; 92(3):431-438.
6. Guéguen P, Rouault K, Chen JM, et al. A missense mutation in the alpha-actinin 1 gene (ACTN1) is the cause of autosomal dominant macrothrombocytopenia in a large French family. *PLoS ONE.* 2013;8(9):e74728.
7. Noris P, Pecci A, Di Bari F, et al. Application of a diagnostic algorithm for inherited thrombocytopenias to 46 consecutive patients. *Haematologica.* 2004;89(10):1219-1225.
8. Balduini CL, Pecci A, Noris P. Diagnosis and management of inherited thrombocytopenias. *Semin Thromb Hemost.* 2013;39(2):161-171.
9. Biino G, Santimone I, Minelli C, et al. Age- and sex-related variations in platelet count in Italy: a proposal of reference ranges based on 40987 subjects' data. *PLoS ONE.* 2013;8(1):e54289.
10. Noris P, Biino G, Pecci A, et al. Platelet diameters in inherited thrombocytopenias: analysis of 376 patients with all known disorders. *Blood.* 2014; 124(6):e4-e10.
11. Provan D, Stasi R, Newland AC, et al. International consensus report on the investigation and management of primary immune thrombocytopenia. *Blood.* 2010;115(2): 168-186.
12. Hou M, Andersson PO, Stockelberg D, Mellqvist UH, Ridell B, Wadenvik H. Plasma thrombopoietin levels in thrombocytopenic states: implication for a regulatory role of bone marrow megakaryocytes. *Br J Haematol.* 1998;101(3): 420-424.
13. Balduini CL, Savoia A, Seri M. Inherited thrombocytopenias frequently diagnosed in adults. *J Thromb Haemost.* 2013;11(6): 1006-1019.

Criteria for evaluating response and outcome in clinical trials for children with juvenile myelomonocytic leukemia

Charlotte M. Niemeyer,[1] Mignon L. Loh,[2] Annamaria Cseh,[1] Todd Cooper,[3] Christopher C. Dvorak,[4] Rebecca Chan,[5] Blanca Xicoy,[6] Ulrich Germing,[7] Seiji Kojima,[8] Atsushi Manabe,[9] Michael Dworzak,[10] Barbara De Moerloose,[11] Jan Starý,[12] Owen P. Smith,[13] Riccardo Masetti,[14] Albert Catala,[15] Eva Bergstraesser,[16] Marek Ussowicz,[17] Oskana Fabri,[18] André Baruchel,[19] Hélène Cavé,[20] Michel Zwaan,[21] Franco Locatelli,[22] Henrik Hasle,[23] Marry M. van den Heuvel-Eibrink,[24] Christian Flotho,[1] and Ayami Yoshimi[1]

[1]Department of Pediatrics and Adolescent Medicine, Division of Pediatric Hematology and Oncology University of Freiburg, Germany; [2]Department of Pediatrics and the Helen Diller Comprehensive Cancer Center, University of California, San Francisco, CA, USA; [3]Aflac Cancer and Blood Disorders Center/Children's Healthcare of Atlanta/Emory University, Atlanta, GA, USA; [4]Division of Pediatric Allergy, Immunology, and Bone Marrow Transplant, Benioff Children's Hospital, University of California, San Francisco, CA, USA; [5]Department of Pediatrics, The Herman B Wells Center for Pediatric Research, Indiana University School of Medicine, Indianapolis, IN, USA; [6]Department of Hematology, Hospital Germans Trias i Pujol and Institut Català d'Oncologia-José Carreras Leukemia Research Institute, Badalona, Spain; [7]Department of Hematology, Oncology and Clinical Immunology, Heinrich-Heine-University, Düsseldorf, Germany; [8]Department of Pediatrics, Nagoya University Graduate School of Medicine, Japan; [9]Department of Pediatrics, St. Luke's International Hospital, Tokyo, Japan; [10]St. Anna Children's Hospital and Children's Cancer Research Institute, Department of Pediatrics, Medical University of Vienna, Austria; [11]Department of Pediatric Hemato-Oncology, Ghent University Hospital, Belgium; [12]Department of Pediatric Hematology and Oncology, Charles University and University Hospital Motol, Czech Pediatric Hematology Working Group, Prague, Czech Republic; [13]Pediatric Oncology and Hematology, Our Lady's Children's Hospital, Crumlin, Dublin, Ireland; [14]Department of Pediatric Oncology and Hematology, University of Bologna, Italy; [15]Department of Hematology, Hospital Sant Joan de Déu, Barcelona, Spain; [16]Department of Hematology and Oncology, University Children's Hospital, Zurich, Switzerland; [17]Department of Pediatric Oncology, Hematology and BMT, Wroclaw Medical University, Poland; [18]Department of Hematology and Transfusiology, Comenius University, Bratislava, Slovakia; [19]Department of Pediatric Hematology of Robert Debré Hospital and Paris Diderot University, Paris, France; [20]Department of Genetics, Hôpital Robert Debré, and Paris Diderot University, Paris, France; [21]ErasmusMC-Sophia Children's Hospital, Erasmus Medical Center, Rotterdam, and the Netherlands and ITCC; [22]Department of Pediatric Hematology and Oncology, Bambino Gesù Children's Hospital, Rome, University of Pavia, Italy; [23]Department of Pediatrics, Aarhus University Hospital Skejby, Aarhus, Denmark; and [24]ErasmusMC-Sophia Children's Hospital, Erasmus Medical Center, Rotterdam, and Dutch Childhood Oncology Group, The Hague, The Netherlands

ABSTRACT

Juvenile myelomonocytic leukemia is a rare myeloproliferative disease in young children. While hematopoietic stem cell transplantation remains the only curative therapeutic option for most patients, children with juvenile myelomonocytic leukemia increasingly receive novel agents in phase I-II clinical trials as pre-transplant therapy or therapy for relapse after transplantation. However, response criteria or definitions of outcome for standardized evaluation of treatment effect in patients with juvenile myelomonocytic leukemia are currently lacking. Here we propose criteria to evaluate the response to the non-transplant therapy and definitions of remission status after hematopoietic stem cell transplantation. For the evaluation of non-transplant therapy, we defined 6 clinical variables (white blood cell count, platelet count, hematopoietic precursors and blasts in peripheral blood, bone marrow blast percentage, spleen size and extramedullary disease) and 3 genetic variables (cytogenetic, molecular and chimerism response) which serve to describe the heterogeneous picture of response to therapy in each individual case. It is hoped that these criteria will facilitate the comparison of results between clinical trials in juvenile myelomonocytic leukemia.

Introduction

Juvenile myelomonocytic leukemia (JMML) is a clonal disease in young children.[1,2] Patients with JMML present with leukocytosis, monocytosis and splenomegaly, features similar to those observed in the myeloproliferative subtype of chronic myelomonocytic leukemia (CMML) in adults.[3] Other clinical signs of JMML include thrombocytopenia, leukemic skin infiltration, elevation of fetal hemoglobin (HbF), and hypersensitivity of hematopoietic progenitors to granulocyte-macrophage colony-stimulating factor (GM-CSF).[4] Approximately 90% of patients with JMML harbor largely mutually exclusive mutations in *PTPN11, NF1, NRAS, KRAS,* or *CBL* in their leukemic cells resulting in hyperactivation of the RAS-MAPK pathway.[5-12]

Hematopoietic stem cell transplantation (HSCT) is still the only curative therapy for the vast majority of JMML patients.[13-15] However, with advances in understanding the underlying molecular mechanisms in JMML, the potential for the introduction of novel therapeutic agents has been recognized for some time. Several molecules, such as isotretinoin, zoledronic acid, and farnesyl transferase inhibitor R115777 have been evaluated in pre-HSCT windows or compassionately used.[16-18] Recently, azacitidine, a DNA-hypomethylating agent, was reported to induce hematologic and molecular remissions in some children with JMML,[19,20] and is currently being tested in clinical trials in Europe. Additional efforts are underway to employ therapeutic inhibition of the MEK/ERK and PI3K pathways.[21-23]

 doi:10.3324/haematol.2014.109892
Manuscript received on May 7, 2014. Manuscript accepted on September 25, 2014.
Correspondence: charlotte.niemeyer@uniklinik-freiburg.de

In order to evaluate the efficacy of any conventional or novel interventions for JMML, standardized criteria to define responses and relapse are urgently required. With the goal of defining widely accepted criteria of response to therapy, international experts from the European Working Groups of Myelodysplastic Syndromes in Childhood (EWOG-MDS), the Children's Oncology Group (COG) from the US, and from the Japanese Society of Pediatric Hematology/Oncology met to find an agreement at the JMML International Symposium, New Orleans, USA, (6 December 2013). The agreed criteria are presented in this manuscript.

Proposal of response criteria in clinical trials of therapy in JMML

Previous efforts for standardized response criteria for non-HSCT therapy in JMML

In adults, standardized response criteria proposed by an International Working Group of MDS have been widely used in clinical trials for MDS as well as CMML.[24,25] These criteria are, however, not applicable to JMML and myeloproliferative CMML because they focus on reduction of blast percentage and improvement of blood counts, and are not designed to evaluate myeloproliferative features such as organomegaly.

Bergstraesser *et al.* defined response criteria in JMML considering white blood cell (WBC) count, platelet count, as well as liver and spleen size.[26] These authors retrospectively evaluated the efficacy of 129 treatment courses other than HSCT administered to 63 children with JMML and reported a significant correlation between WBC count or spleen size and the efficacy of non-HSCT therapy. This finding was later applied to response criteria proposed by Chan *et al.* describing complete response (WBC <20x10^9/L and normalization of spleen size) and partial response (<50% of initial WBC but total still greater than 20x10^9/L and 25% decrease in spleen size from initial size) based solely on these two criteria, WBC count and spleen size.[27] Due to the rarity of JMML there is no published prospective clinical trial that has actually applied these criteria, and there are evident limitations when only these two variables are used. The definitions are only applicable in patients with leukocytosis (WBC ≥20x10^9/L) and splenomegaly (≥2 cm below the costal margin). However, among 497 JMML patients currently registered in the EWOG-MDS studies, 30% had a WBC count less than 20x10^9/L, and 12% a spleen size of less than 2 cm below the costal margin at diagnosis (*EWOG-MDS, unpublished data, 2014*). In addition, the criteria are not applicable to patients relapsing post HSCT who have reappearance of cytogenetic or molecular abnormalities after HSCT but who do not yet show the full clinical picture of relapse. Response criteria thus need to be applicable in many different clinical situations for a broad range of patients. Therefore, clinical variables other than WBC count and spleen size are needed, and cytogenetic and molecular variables are also necessary to describe disease status.

The concept behind the proposed response criteria

As outlined above, response measurements in JMML need to be applicable to the highly heterogeneous clinical features at presentation and to individual response patterns to different therapeutic agents. Therefore, 6 clinical variables and 3 genetic variables were selected (Table 1). For each of these variables (v), complete response (vCR), partial response (vPR) and progressive disease (vPD) are defined. This makes the evaluation of heterogeneous effects of each intervention possible. Because we recognize that each patient can present with different clinical, cytogenetic and molecular features, the number of evaluable variables at the start of therapy differs among patients. Based on the cumulative response of these 9 variables, the clinical and genetic remission status can be described (Tables 2).

Variables to evaluate response

In addition to WBC count and spleen size, clinical variables include presence of myeloid/erythroid precursors and blasts in peripheral blood, platelet count, percentage of blasts in bone marrow, and presence of extramedullary disease (Table 1).[4] Two additional hallmarks of JMML, the level of hemoglobin F (HbF) corrected for age and the presence of monocytosis, have intentionally been excluded as response criteria for various reasons. High HbF levels at diagnosis are known to predict outcome but are dependent on karyotype.[4] Moreover, so far there has been no report on serial HbF levels during the natural course of JMML or following HSCT. Therefore, further studies to evaluate HbF during the clinical course of JMML patients are necessary. Monocytosis more than 1.0x10^9/L is one of the diagnostic criteria of JMML,[4] but the absolute monocyte count generally correlates with the WBC. Since the usefulness of the WBC count has been previously confirmed, we chose the WBC count, but not the monocyte count, as a variable to be evaluated.[26] Moreover, monocytosis can be non-specific since it is observed in various conditions, such as infections or an early sign of bone marrow recovery after HSCT, and leukocytosis in JMML is manifested not only by monocytosis but also by circulating immature myeloid cells in the peripheral blood.

Since the spleen size is one of the variables evaluating treatment efficacy in JMML,[26] reliable methods to measure the size of this variably shaped organ are required. Size determination by palpation with measurement of the length between the spleen tip and the left costal margin is clinically appropriate[26,28-30] but may not be sufficient for clinical trials since its results are not verifiable. Measurements by computed tomography are to be avoided in children with JMML because of radiation issues, and magnetic resonance imaging generally requires deep sedation or anesthesia. For these reasons, we currently recommend evaluation of spleen size by ultrasound with the linear measurement of the splenic length, defined as the maximum distance between the dome and the tip of spleen in the right lateral decubitas position.[31]

The three genetic variables selected for evaluating response were cytogenetics, molecular alterations, and chimerism. Cytogenetic and molecular data must have been collected at diagnosis while chimerism is only applicable after HSCT. Abnormal karyotypes are observed in approximately 35% of JMML patients, with monosomy 7 being the most common aberration (25%).[4] Oncogenic molecular alterations in *PTPN11, NF-1, NRAS, KRAS* or *CBL*, noted in approximately 90% of patients are increasingly important tools for diagnosis and follow up of JMML.[5-12] We anticipate that additional somatic mutations will be discovered in JMML. Indeed, recently *SETBP1* and *JAK3* mutations were reported as a result of an exome sequencing project.[32] However, until these markers are fur-

ther validated, we would suggest that these mutations, which might indicate sub-clones, fall under the category of "acquired molecular abnormalities". Analysis of donor chimerism has been a standard measurement to follow JMML patients given allogeneic HSCT. While discussion of the various methods used to determine donor chimerism is beyond the scope of this consensus report, there was broad agreement that unsorted cell donor chimerism should be a common measurement in clinical trials. Most JMML patients with persistent mixed chimerism experience clinical relapse of JMML,[33] and are thus candidates for early intervention with innovative therapies prior to development of a full clinical relapse.

Definitions of response to therapy other than HSCT in JMML

Based on the response of each applicable variable listed in Table 1, the clinical and genetic remission status can be

Table 1. Variables for evaluation of response to therapy in JMML.

Variables for response		Definition of response		Definition of disease progression or relapse (applicable to all patients)
	Assessment of CR and PR is feasible if the following are present before therapy	Requirement for CR for each variable (vCR)	Requirement for PR for each variable (vPR)	Requirement for PD for each variable (vPD)
Clinical variables				
1) WBC count	>20×10⁹/L	3.0-15.0×10⁹/L	Decreased by ≥50% over pretreatment but still >15×10⁹/L	Increase by ≥50% and ≥20×10⁹/L
2) Myeloid and erythroid precursors and blasts in PB*	≥ 5%	0-1%	Decreased by ≥50% over pre-treatment but still ≥ 2%	Increase from the baseline: < 5%: ≥ 50% increase and ≥ 5% ≥ 5%: ≥ 50% increase of total % of myeloid and erythroid precursors and blasts
3) Platelet count	<100×10⁹/L	≥100×10⁹/L	For patients starting with ≥ 20×10⁹/L platelets: absolute increase of ≥ 30×10⁹/L For patients starting with < 20 ×10⁹/L platelets: increase by ≥ 100% and > 20×10⁹/L	Development of transfusion dependency or if patients have the baseline of the platelet count of ≥30×10⁹/L, decrease by ≥50% and <100×10⁹/L
4) BM blasts	≥5%	<5%	Decreased by ≥50% over pre-treatment but still ≥5%	Increase from baseline; < 5%: ≥ 50% increase and ≥ 5% ≥ 5%: ≥ 50% increase of BM blasts
5) Spleen size a) Clinical evaluation or	≥2 cm under the costal margin	No splenomegaly	50% decrease by cm under the costal margin	Increase by ≥100% if baseline <4cm from under the costal margin ≥50% if baseline 5-10 cm >30% if baseline >10 cm
b) Sonography	Length of spleen ≥ 150% of upper limit of normal range	No splenomegaly	>25% decrease by length, but still splenomegaly	Increase by ≥25% of length
6) Extramedullary disease#	Extramedullary leukemic infiltration	No evidence of extramedullary leukemic infiltration in any organ	–	Worsening or new lesions of extramedullary leukemic infiltration
7) Cytogenetic response	Somatic cytogenetic abnormality detected	Normal karyotype	–	Reappearance or additional acquirement of cytogenetic abnormalities
8) Molecular response	Somatic genetic anomalies detected **	Absence of somatic genetic anomalies	–	Reappearance or additional acquirement of JMML-specific somatic gene abnormalities
9) Chimerism response (only for patients after HSCT)	>15% autologous cells after allo-HSCT	Complete donor chimerism	–	50% increase and >5% increase of autologous cells and >5%

*CR: complete response; PR: partial response; PD: progressive disease; WBC: white blood cell; PB: peripheral blood; BM: bone marrow. *Myeloid precursors include promyelocytes, myelocytes and metamyelocytes. The myeloid and erythroid precursors and blasts in PB are given as percentage of the total nucleated cells in PB (WBC including erythroblasts). **In* NF-1, PTPN11, NRAS, KRAS, *or* CBL, *thus the mutations are thought to be initiating. In patients with germ-line* NF-1, PTPN11 *or* CBL *mutation, only acquired mutations can be evaluated for response and relapse after therapy. The germ-line mutation remains even if patients achieved complete molecular response. #Extramedullary disease includes infiltration of skin, lung, and, very rarely, cranial nerves or central nervous system.*

defined for each patient (Table 2). In patients who achieve genetic complete remission (gCR), JMML cells are considered to have been eradicated, irrespective of clinical remission status. Patients with gCR may have persistent splenomegaly or leukocytosis from causes other than JMML, such as infections. However, it is unlikely that such a patient has clinical signs of progressive disease of JMML in the presence of gCR. In such a patient, any new clonal abnormalities, other possible errors of genetic examinations, or other disorders which give rise to JMML-like clinical features, should be excluded.

Response criteria for clinical trials of HSCT

There is a consensus that criteria for remission after HSCT are somewhat different from those stated above for remission after non-HSCT. The remission criteria in HSCT recipients include the results of chimerism analyses (Table 3). Appraisal of methodological consideration of chimerism studies will change over time and is beyond the scope of this consensus document. Patients undergoing HSCT who achieve neutrophil engraftment and complete donor chimerism with disappearance of acquired cytogenetic and molecular abnormalities are considered to have a complete remission of JMML. In these individuals, complete remission is defined irrespective of the spleen size or WBC counts, since post HSCT, patients often have persistent splenomegaly and leukocytosis without active JMML due to infections, graft-*versus*-host disease or other hepatic complications. For the very few cases with mixed chimerism after HSCT and no diagnostic cytogenetic or molecular marker, definition of complete remission requires the resolution of all clinical features indicative of JMML (Table 3).

Table 2. Definition of response following therapy other than HSCT in JMML.

Clinical remission status: variable 1-6 in Table 1		Genetic remission status: variable 7-9 in Table 1	
Clinical complete remission (cCR)	Patient fulfills the criteria of CR of all applicable clinical variables 1-6 of Table 1 The response variables must be maintained for at least 4 weeks.	**Genetic complete remission (gCR)**	Defined if the patient shows a normal karyotype and absence of acquired mutations in *PTPN11*, *NF-1*, *NRAS*, *KRAS*, or *CBL*.
Clinical partial remission (cPR)	Defined if the patient does not fulfill the criteria of cCR, but vPR was achieved in at least one of clinical variables (1-6) and none of clinical variables showed vPD.	–	–
Clinical stable disease (cSD)	Defined if the patient does not fulfill the criteria of cCR and cPR, but none of the variables showed vPD.	**Genetic stable disease (gSD)**	Defined if the patient does not fulfill the criteria of gCR, but none of the genetic variables (7-9) showed vPD.
Clinical progressive disease (cPD)	Defined if any of the variables 1-6 showed vPD.	**Genetic progressive disease (gPD)**	Defined if any of the variables 7-9 showed vPD.
Clinical relapse (cRel)	Defined if any of the variables 1-6 showed vPD after the achievement of cCR or cPR.	**Genetic relapse (gRel)**	Reappearance of an abnormal karyotype and/or mutation of genes related with JMML if previously undetected, and/or (only for patients after HSCT) increase in recipient chimerism with at least 10% of autologous cells and >50% increase above the baseline.

***In patients with germ-line* NF-1, PTPN11 *or* CBL *mutation, the germ-line mutation remains even if patients achieved a genetic complete remission.*

Table 3. Definition of complete remission and relapse after hematopoietic stem cell transplantation in children with JMML.

Complete remission is defined in the presence of neutrophil engraftment and:
1. full donor chimerism of unsorted cells from PB or BM and
2. disappearance of acquired cytogenetic and molecular abnormalities in patients with such a previously identified abnormality

For patients without cytogenetic or acquired molecular abnormalities at diagnosis, who do not achieve full donor chimerism (as defined above), all of the following features of clinical remission must be achieved for definition of complete remission:
a. absence of splenomegaly on exam and imaging, if splenomegaly was present at diagnosis
b. absolute leukocyte count < 15×10^9/L
c. blasts in BM of <5%,
d. myeloid/erythroid precursors including blasts in PB ≤1%

Relapse is defined if one of the following criteria is fulfilled:
1. clinical JMML features and mixed chimerism >5%
2. blasts in BM ≥5%, total blasts and myeloid/erythroid precursors in PB ≥5%*
3. cytogenetic relapse: if applicable, reappearance of clonal cytogenetic abnormality
4. molecular relapse: if applicable, reappearance of acquired genetic anomalies

*PB: peripheral blood; BM: bone marrow. *Exclude other causes of appearance of blasts and myeloid/erythroid precursors in PB such as the regenerating phase after engraftment, severe infections and effect of granulocyte-colony-stimulating factor.*

Conclusion

In this paper we propose response and relapse criteria for patients who are diagnosed and treated for JMML, recognizing the complexities of disease presentation and therapeutic interventions. The usefulness and suitability of these criteria need to be proven in prospective clinical trials. It is likely that the proposed response criteria will require modifications in the future based on the accumulated experiences and advances of molecular biology in JMML. Because the goal of therapy of children with JMML is a cure, it is also important to be aware that responses need to be translated into an increase in long-term survival in well-controlled clinical trials.

Acknowledgments

We thank the JMML Foundation for their continuous efforts to nurture the discussion among clinicians and scientists working in the field of JMML and organizing an annual International JMML Symposium. The project described here was supported by award number R13CA132568 from the National Cancer Institute to the JMML Foundation. The content is solely the responsibility of the authors and does not necessarily represent the official views of the National Cancer Institute or the National Institutes of Health. This project was also supported by a grant from the Parent Initiative for Children with Cancer, Freiburg (Förderverein für krebskranke Kinder e.V. Freiburg i. Br.) to the Coordinating Study Center of the EWOG-MDS in Freiburg, Germany.

Authorship and Disclosures

Information on authorship, contributions, and financial & other disclosures was provided by the authors and is available with the online version of this article at www.haematologica.org.

References

1. Niemeyer CM, Kratz CP. Paediatric myelodysplastic syndromes and juvenile myelomonocytic leukaemia: molecular classification and treatment options. Br J Haematol. 2008;140 (6):610-24.
2. Loh ML. Recent advances in the pathogenesis and treatment of juvenile myelomonocytic leukaemia. Br J Haematol. 2011; 152(6):677-87.
3. Bennett JM, Catovsky D, Daniel MT, Flandrin G, Galton DA, Gralnick H, et al. The chronic myeloid leukaemias: guidelines for distinguishing chronic granulocytic, atypical chronic myeloid, and chronic myelomonocytic leukaemia. Proposals by the French-American- British Cooperative Leukaemia Group. Br J Haematol. 1994; 87(4):746-54.
4. Niemeyer CM, Arico M, Basso G, Biondi A, Cantu RA, Creutzig U, et al. Chronic myelomonocytic leukemia in childhood: a retrospective analysis of 110 cases. European Working Group on Myelodysplastic Syndromes in Childhood (EWOG-MDS). Blood. 1997;89(10):3534-43.
5. Tartaglia M, Niemeyer CM, Fragale A, Song X, Buechner J, Jung A, et al. Somatic PTPN11 mutations in juvenile myelomonocytic leukemia, myelodysplastic syndromes and acute myeloid leukemia. Nat Genet. 2003; 34(2):148-50.
6. Kratz CP, Niemeyer CM, Castleberry RP, Cetin M, Bergsträsser E, Emanuel PD, et al. The mutational spectrum of PTPN11 in juvenile myelomonocytic leukemia and Noonan syndrome/myeloproliferative disease. Blood. 2005;106(6):2183-5.
7. Miyauchi J, Asada M, Sasaki M, Tsunematsu Y, Kojima S, Mizutani S. Mutations of the N-ras gene in juvenile chronic myelogenous leukemia. Blood. 1994;83(8):2248-54.
8. Side LE, Emanuel PD, Taylor B, Franklin J, Thompson P, Castleberry RP, et al. Mutations of the NF1 gene in children with juvenile myelomonocytic leukemia without clinical evidence of neurofibromatosis, type 1. Blood. 1998;92(1):267-72.
9. Flotho C, Valcamonica S, Mach-Pascual S, Schmahl G, Corral L, Ritterbach J, et al. Ras mutations and clonality analysis in children with juvenile myelomonocytic leukemia (JMML). Leukemia. 1999;13(1):32-7.
10. Loh ML, Sakai DS, Flotho C, Kang M, Fliegauf M, Archambeault S, et al. Mutations in CBL occur frequently in juvenile myelomonocytic leukemia. Blood. 2009; 114(9):1859-63.
11. Niemeyer CM, Kang MW, Shin DH, Furlan I, Erlacher M, Bunin NJ, et al. Germline CBL mutations cause developmental abnormalities and predispose to juvenile myelomonocytic leukemia. Nat Genet. 2010;42(9):794-800.
12. de Vries AC, Zwaan CM, van den Heuvel-Eibrink MM. Molecular basis of juvenile myelomonocytic leukemia. Haematologica. 2010; 95(2):179-82.
13. Locatelli F, Nöllke P, Zecca M, Korthof E, Lanino E, Peters C, et al. Hematopoietic stem cell transplantation (HSCT) in children with juvenile myelomonocytic leukemia (JMML): results of the EWOG-MDS/EBMT trial. Blood. 2005;105(1):410-9.
14. Yabe M, Sako M, Yabe H, Osugi Y, Kurosawa H, Nara T, et al. A conditioning regimen of busulfan, fludarabine, and melphalan for allogeneic stem cell transplantation in children with juvenile myelomonocytic leukemia. Pediatr Transplant. 2008; 12(8):862-7.
15. Locatelli F, Crotta A, Ruggeri A, Eapen M, Wagner JE, Macmillan ML, et al. Analysis of risk factors influencing outcomes after cord blood transplantation in children with juvenile myelomonocytic leukemia: a EUROCORD, EBMT, EWOG-MDS, CIBMTR study. Blood. 2013;122(12):2135-41.
16. Castleberry RP, Emanuel PD, Zuckerman KS, Cohn S, Strauss L, Byrd RL, et al. A pilot study of isotretinoin in the treatment of juvenile chronic myelogenous leukemia. N Engl J Med. 1994;331(25):1680-4.
17. Castleberry RP, Loh ML, Jayaprakash N, Peterson, A., Casey, V., Chang, M, et al. Phase II window study of the farnesyltransferase inhibitor R115777 (Zarnestra®) in untreated juvenile myelomonocytic leukemia (JMML): A Children's Oncology Group study [abstract]. Blood. 2005; 106:727a.
18. Shimada H, Shima H, Shimasaki N, Yoshihara H, Mori T, Takahashi T. Little response to zoledronic acid in a child of juvenile myelomonocytic leukemia (JMML) harboring the PTPN11 mutation. Ann Oncol. 2005;16(8):1400.
19. Furlan I, Batz C, Flotho C, Mohr B, Lübbert M, Suttorp M, et al. Intriguing response to azacitidine in a patient with juvenile myelomonocytic leukemia and monosomy 7. Blood. 2009;113(12):2867-8.
20. Cseh A, Niemeyer CM, Catalá A, Dworzak M, Hasle H, van den Heuvel-Eibrink MM, et al. Therapy with azacitidine in pediatric MDS and JMML A retrospective survey of the EWOG-MDS study. Haematologica. 2012;97:S3.
21. Lyubynska N, Gorman MF, Lauchle JO, Hong WX, Akutagawa JK, Shannon K, et al. A MEK inhibitor abrogates myeloproliferative disease in Kras mutant mice. Sci Transl Med. 2011;3:76ra27.
22. Chang T, Krisman K, Theobald EH; Xu J, Akutagawa J, Lauchle JO, et al. Sustained MEK inhibition abrogates myeloproliferative disease in Nf1 mutant mice. J Clin Invest. 2013;123(1):335-9.
23. Goodwin CB, Li XJ, Mali RS, Chan G, Kang M, Liu Z et al. PI3K p110delta uniquely promotes gain-of-function Shp2-induced GM-CSF hypersensitivity in a model of JMML. Blood. 2014;23(18):2838-42.
24. Cheson BD, Bennett JM, Kantarjian H, Pinto A, Schiffer CA, Nimer SD, et al. Report of an international working group to standardize response criteria for myelodysplastic syndromes. Blood. 2000;96(12):3671-4.
25. Cheson BD, Greenberg PL, Bennett JM, Lowenberg B, Wijermans PW, Nimer SD, et al. Clinical application and proposal for modification of the International Working Group (IWG) response criteria in myelodysplasia. Blood. 2006;108(2):419-25.
26. Bergstraesser E, Hasle H, Rogge T, Fischer A, Zimmermann M, Noellke P, et al. Non-hematopoietic stem cell transplantation treatment of juvenile myelomonocytic leukemia: a retrospective analysis and definition of response criteria. Pediatr Blood Cancer. 2007;49(5):629-33.
27. Chan RJ, Cooper T, Kratz CP, Weiss B, Loh ML. Juvenile myelomonocytic leukemia: a report from the 2nd International JMML Symposium. Leuk Res. 2009;33(3):355-62.
28. Ades L, Sekeres MA, Wolfromm A, Teichman ML, Tiu RV, Itzykson R, et al. Predictive factors of response and survival among chronic myelomonocytic leukemia patients treated with azacitidine. Leuk Res. 2013;37(6):609-13.
29. Aribi A, Borthakur G, Ravandi F, Shan J,

Davisson J, Cortes J, et al. Activity of decitabine, a hypomethylating agent, in chronic myelomonocytic leukemia. Cancer. 2007;109(4):713-7.
30. Wattel E, Guerci A, Hecquet B, Economopoulos T, Copplestone A, Mahé B, et al. A randomized trial of hydroxyurea versus VP16 in adult chronic myelomonocytic leukemia. Groupe Francais des Myelodysplasies and European CMML Group. Blood. 1996;88(7):2480-7.
31. Lamb PM, Lund A, Kanagasabay RR, Martin A, Webb JA, Reznek RH, et al. Spleen size: how well do linear ultrasound measurements correlate with three-dimensional CT volume assessments? Br J Radiol. 2002; 75(895):573-7.
32. Sakaguchi H, Okuno Y, Muramatsu, Yoshida K, Shiraishi Y, Takahashi M, et al. Exome sequencing identifies secondary mutations of SETBP1 and JAK3 in juvenile myelomonocytic leukemia. Nat Genet. 2013;45(8):937-41.
33. Yoshimi A, Niemeyer CM, Bohmer V, Duffner U, Strahm B, Kreyenberg H, et al. Chimaerism analyses and subsequent immunological intervention after stem cell transplantation in patients with juvenile myelomonocytic leukaemia. Br J Haematol. 2005;129(4):542-9.